2005

Sulfur and oxygen isotopic record in sulfate and sulfide minerals of early, deep, pre-Main Stage porphyry Cu–Mo and late Main Stage base-metal mineral deposits, Butte district, Montana

C.W. Field
Oregon State University

L. Zhang
Oregon State University

J.H. Dilles
Oregon State University

Robert O. Rye
U.S. Geological Survey, rrye@usgs.gov

M.H. Reed
University of Oregon

ELSEVIER

Chemical Geology 215 (2005) 61–93

CHEMICAL GEOLOGY
INCLUDING
ISOTOPE GEOSCIENCE

www.elsevier.com/locate/chemgeo

Sulfur and oxygen isotopic record in sulfate and sulfide minerals of early, deep, pre-Main Stage porphyry Cu–Mo and late Main Stage base-metal mineral deposits, Butte district, Montana

C.W. Field[a,*], L. Zhang[a], J.H. Dilles[a], R.O. Rye[b], M.H. Reed[c]

[a]*Department of Geosciences, Oregon State University, Corvallis, OR 97331, USA*
[b]*U.S. Geological Survey, MS-963, Denver Federal Center, P.O. Box 25046, Denver, CO 80225, USA*
[c]*Department of Geological Sciences, University of Oregon, Eugene, OR 97403, USA*

Accepted 1 June 2004

Abstract

Typical porphyry-type Cu–Mo mineralization occupies two connected domal centers, the eastern Pittsmont and western Anaconda domes, that predate and largely underlie the well-known, throughgoing, Main Stage polymetallic veins of Butte. Among the sulfur-bearing minerals recovered from deep drill core of this early pre-Main Stage hydrothermal assemblage are anhydrite, chalcopyrite, pyrite, and molybdenite in veinlets bordered by K-silicate alteration, and pyrite from slightly younger quartz–pyrite veinlets with 'gray-sericitic' alteration selvages. The ranges of $\delta^{34}S$ values for minerals of the K-silicate assemblage are 9.8–18.2‰ for anhydrite (n=23 samples), 3.0‰ to 4.7‰ for molybdenite (n=6), 0.4‰ to 3.4‰ for pyrite (n=19), and −0.1‰ to 3.0‰ for chalcopyrite (n=13). Sulfate–sulfide mineral fractionation is consistent with an approach to isotopic equilibrium, and calculated temperatures for mostly coexisting anhydrite–sulfide pairs (anhydrite–molybdenite, n=6, 545 to 630 °C; anhydrite–pyrite, n=13, 360 to 640 °C; and anhydrite–chalcopyrite, n=8, 480 to 575 °C) are broadly consistent with petrological, alteration, and fluid-inclusion temperature estimates. The $\delta^{34}S$ values for pyrite (n=25) in veinlets of the 'gray-sericitic' assemblage range from 1.7‰ to 4.3‰. The $\delta^{34}S$ values for sulfides of the pre-Main Stage K-silicate and 'gray-sericitic' assemblages are similar to those of most Main Stage sulfides, for which 281 analyses by other investigators range from −3.7‰ to 4.8‰. Sulfide–sulfide mineral pairs provide variable (−175 to 950 °C) and less reliable temperature estimates that hint of isotopic disequilibria.

The sulfide data, alone, suggest a conventionally "magmatic" value of about 1‰ or 2‰ for Butte sulfur. However, the high modal mineral ratios of sulfate/sulfide, and the isotopic systematics of the early K-silicate assemblage, suggest that pre-Main Stage fluids may have been sulfate-rich ($X_{SO_4^{2-}} \approx 0.75$) and that total sulfur was isotopically heavy ($\delta^{34}S_{\Sigma S} \approx 10‰$), which would have required an evaporitic crustal component to the relatively oxidized granitic parental magma that was the source of the hydrothermal fluids and sulfur. Modeling of brine–vapor unmixing of a 10‰ fluid, reduction of sulfate, and vapor loss suggest that these processes may have formed the isotopically heavier (14‰ to 18‰) anhydrite of the western and shallower Anaconda Dome, contrasting with the lighter and more numerous values (9.8‰ to 12.9‰) for anhydrite of the eastern and

* Corresponding author. Tel.: +1 541 574 6239; fax: +1 541 737 1200.
E-mail address: fieldc@geo.oregonstate.edu (C.W. Field).

0009-2541/$ - see front matter
doi:10.1016/j.chemgeo.2004.06.049

deeper Pittsmont Dome. Such a process might also have been able to produce the sulfide isotopic compositions of the younger 'gray-sericitic' and Main Stage zones, but the limited data for sulfates permit $\delta^{34}S_{\Sigma S}$ compositions of either 2‰ or 10‰ for these later fluids. Oxygen isotopic data for late Main Stage barite (−0.3‰ to 12.4‰, n=4 samples) confirm variable meteoric water contributions to these fluids, and the data support either the absence of, or limited, sulfate–sulfide isotopic equilibrium in these samples. The $\delta^{34}S$ values for sulfate–sulfur of barite are markedly variable (4.4‰ to 27.3‰), and the unusual ^{34}S depletion indicates sulfur formed by oxidation of H_2S.

Keywords: Butte, Montana; Porphyry Cu–Mo deposit; Sulfur isotopes; Sulfate–sulfide assemblages; Oxygen isotopes; Contamination

1. Introduction

The Butte mining district in southwestern Montana is preeminent not only as a major U.S. producer of hydrothermal Cu–Pb–Zn–Mn–Ag ores for nearly 130 years, but also as the prominent residence of rogues and heros involved in notorious mineral litigation near the close of the Nineteenth Century. In addition, for 90 years or more, the district has been the location of numerous industry, government, and university investigations directed to applied and basic ore-deposit research. Several of the investigations include the applications of stable isotopes to questions relating to ore genesis, and those of sulfur represent an early and recurring subject. Most of the previous sulfur-isotope research has been concerned almost exclusively with the large, throughgoing veins related to the well-known Main Stage mineralization. In contrast, our present study is largely directed to the earlier, deeper, and higher temperature pre-Main Stage porphyry Cu–Mo mineralization. The sulfur-bearing minerals analyzed are those contained in: (a) thin quartz–anhydrite–sulfide veinlets bordered by 'early dark micaceous' selvages and more pervasive K-silicate alteration assemblages, (b) quartz–pyrite–chalcopyrite veinlets bordered by pale green sericitic and dark green sericitic alteration selvages, both of which are part of the early K-silicate alteration suite, and (c) the slightly younger quartz–pyrite veinlets with gray-sericitic alteration selvages. Samples were selected from diamond-drill core obtained by Anaconda in 1979–1981 as part of a deep exploration program at Butte. Our sample suite also includes four examples of barite–pyrite vein fillings from late Main Stage mineralization.

The principal objectives of this investigation were to (1) compare the $\delta^{34}S$ systematics of early pre-Main Stage mineralization to that of the later Main Stage event; (2) establish the extent to which isotopic equilibrium was approached between different sulfur-bearing minerals and, thus, the apparent reliability of isotopic temperatures derived therefrom; (3) estimate the isotopic composition of total sulfur ($\delta^{34}S_{\Sigma S}$) in the Butte hydrothermal system and thereby gain better insight as to the likely source(s) of this sulfur; and (4) undertake a reconnaissance oxygen-isotope study of the early high-temperature anhydrite and the late low-temperature barite. Parts of this research have been reported by Zhang et al. (1999), Zhang (2000), and Field et al. (2000). Interpretations of our data have benefited greatly from recent and ongoing geochemical studies of pre-Main Stage mineralization, from previous isotopic studies of Main Stage mineralization, from recent geological studies of pre-Main Stage mineralization, and from continued improvements in the understanding of sulfur-isotope fractionation effects.

2. Geological setting

Mineral deposits of the Butte district are located near the southern end of the Late Cretaceous Boulder batholith, which was emplaced into a package consisting of clastic sedimentary rocks of the middle Proterozoic Belt Supergroup, a thin overlying sequence of Paleozoic platform-carbonate and clastic rocks, and upper Cretaceous Elkhorn Mountains Volcanics (Schmidt et al., 1990). The upper part of the Belt includes carbonates, stromatolites, and red-bed siltstones and mudstones of the Missoula Group that are indicative of shallow marine to supratidal conditions and locally contain salt casts (cf. Smith and Barnes, 1966). Marine to supratidal conditions occur in the

Helena embayment where the Boulder batholith was emplaced, and marine to subareal clastic sedimentary rocks crop out along the Belt-age Willow Creek Fault in the Highland Mountains, 20 km southeast of Butte (O'Neill, 1995). Ores are hosted by the Butte Quartz Monzonite, the dominant intrusive phase of the batholith. Detailed petrographic studies and field descriptions of the Butte Quartz Monzonite indicate a relatively uniform mineral content that is dominated, in order of diminishing abundance by plagioclase, quartz, K-feldspar, biotite, and hornblende, with accessory magnetite, titanite, ilmenite, apatite, and zircon (Weed, 1912; Sales, 1914; Klepper et al., 1957; Becraft et al., 1963; Ruppel, 1963; Tilling, 1964; Smedes, 1966; Meyer et al., 1968; Robson, 1971; Roberts, 1975; Brimhall, 1977; Brownlow and Kurz, 1979). Trace amounts of Cu–Fe sulfides, but never sulfate minerals, are sparingly present in unaltered Butte Quartz Monzonite. Hornblende barometry (Dilles et al., 1999) indicates that the present exposures in the district represent original depths of 7 to 8 km, which are consistent with fluid-inclusion pressure estimates of the pre-Main Stage hydrothermal event (Roberts, 1975).

Pre-Main Stage mineralization at Butte is defined collectively by the types and zonations of metals and of ore, gangue, and alteration minerals. The stage consists of typical porphyry-type, fracture-controlled, Cu–Mo mineralization that predates and largely underlies the throughgoing Main Stage polymetallic veins for which the district is famous. This mineralization occupies two centers, a western Anaconda Dome and an eastern Pittsmont Dome, that trend about N80°W and straddle a swarm of quartz porphyry dikes (Fig. 1). Although the Pittsmont Dome is the larger of the two, both contain identical types of alteration and vein–mineral assemblages related to Cu–Mo mineralization (Reed, 1979). Available evidence suggests that the domes were coeval and originally contiguous, and that they formed prior to the pre-Main Stage gray-sericitic and Main Stage hydrothermal events. The shapes of the two domes are defined by zones of anomalously high concentrations of Mo and Cu, magnetite veinlets, and K-silicate alteration (Fig. 1), which collectively represent the earliest of the pre-Main Stage mineralization at Butte. The associated high-temperature K-silicate alteration is characterized by pervasively biotitized hornblende (Roberts, 1975) and 'early dark micaceous' veinlets (Meyer, 1965) that contain pyrite, chalcopyrite (bulk rock assays of about 0.5 to 0.8 wt.% Cu), molybdenite, anhydrite, magnetite, biotite, K-feldspar, quartz, and other silicates that formed at 550 to 600 °C (Brimhall, 1977). Pervasively biotitized Butte Quartz Monzonite is characterized by the total replacement of magmatic hornblende by hydrothermal biotite, destruction of titanite to a mixture of Fe–Ti oxides, quartz, and anhydrite (Roberts, 1975), partial conversion of plagioclase to K-feldspar, and the introduction of disseminated chalcopyrite, pyrite, and anhydrite, and thus represents typical K-silicate alteration. Most veinlets that accompany K-silicate alteration are dominated by quartz and may contain smaller and variable amounts of anhydrite and molybdenite±chalcopyrite or pyrite±chalcopyrite. Modal analyses (Roberts, 1975; Brimhall, 1977) indicate that altered Butte Quartz Monzonite contains up to 5 vol.% anhydrite and about 2 vol.% sulfides. A second type of alteration assemblage grades outward and upward from the K-silicate zone into a contemporaneous to slightly younger succession of pale green 'sericite', dark green 'sericite'–chlorite, and more distal propylitic epidote–chlorite assemblages of pre-Main Stage alteration (Page, 1979; Reed, 1979). This alteration is accompanied by a second generation of pre-Main Stage veinlets consisting of quartz with locally abundant molybdenite that cut the 'early dark mica' and pale green 'sericite' and veinlets, and corresponds to the zones of high Mo assays in the Anaconda and Pittsmont domes as well as to a deeper area of abundant "barren quartz" veinlets encountered in deep drillholes 1A and 7 (Fig. 1B). [The term 'sericite' generally refers to a fine-grained white mica; however, the composition is unspecified, and the International Mineralogical Association has ruled the use of the term as a mineral name is to be discouraged (Rieder et al., 1998).] Nonetheless, 'sericite' is an abundant and pervasive product of hydrothermal systems, particularly at Butte, where it has been identified as 1*M* and 2*M* muscovite in Main Stage alteration (Meyer et al., 1968).

Main Stage veins that cut pre-Main Stage mineralization are abundant and well-developed in the northern and western parts of the Anaconda Dome. However, these veins are much smaller and fewer in number in the Pittsmont Dome area to the east.

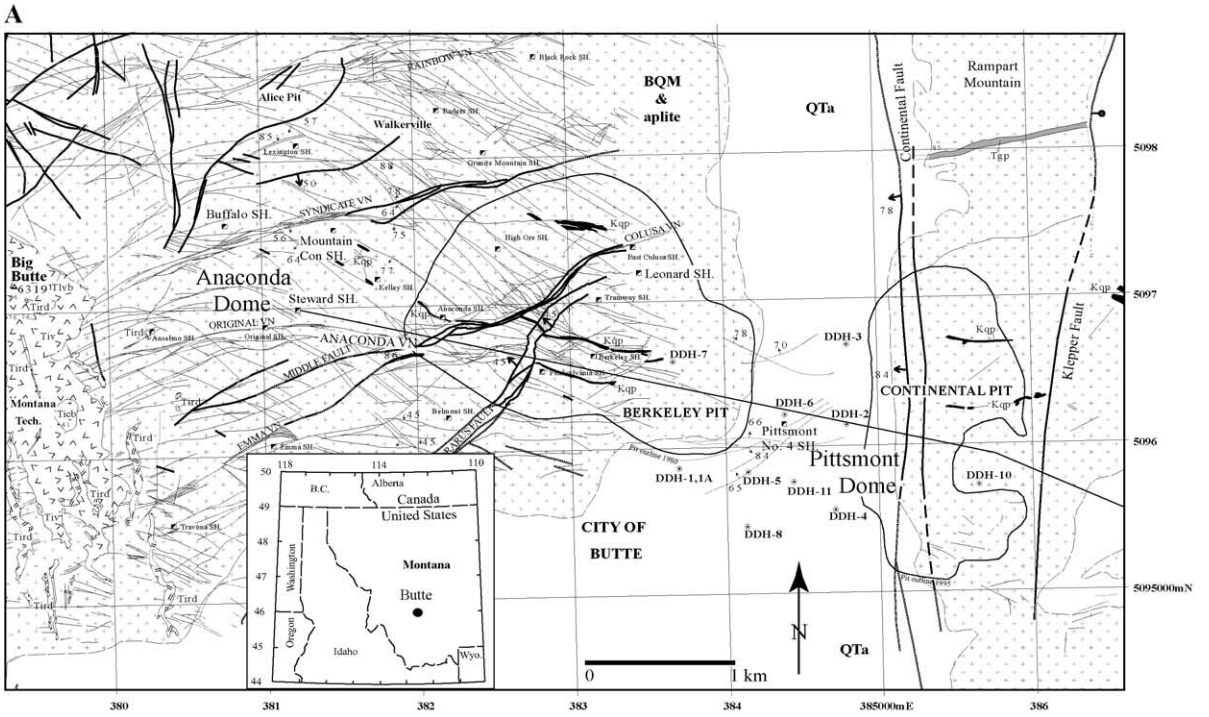
A
BQM & aplite
QTa
Rampart Mountain
Continental Fault
Klepper Fault
Alice Pit
Walkerville
Buffalo SH.
SYNDICATE VN
Mountain Con SH.
Big Butte
Anaconda Dome
Steward SH.
ORIGINAL VN
ANACONDA VN
MIDDLE FAULT
COLUSA VN
Leonard SH.
DDH-3
DDH-7
CONTINENTAL PIT
BERKELEY PIT
DDH-6
DDH-2
Pittsmont No. 4 SH.
Pittsmont Dome
DDH-1,1A
DDH-5
DDH-11
DDH-10
DDH-4
DDH-8
CITY OF BUTTE
Montana Tech.
Canada
United States
Montana
Butte
Idaho
N
0
1 km
5098
5097
5096
5095000mN
380
381
382
383
384
385000mE
386
B
A Anaconda Dome
S77°E
Berkeley Pit
(1979)
Pittsmont Dome
Continental Pit
(approx. limit 2000)
N68°W A'
N77W
S68E
Steward Shaft
Kelly Shaft proj 300 m S
Section 32000 E
Section 36000 E
DDH7 (11170)
DDH6 (11169)
DDH2 (11135)
DDH10 (11172) proj 680 ft S
Alluvium
10759-336
10854-643
Quartz Porphyry Dike
10778-4
10772-31
Sparse GS
Pervasive GS alteration
Magnetite vein (Cu) zone
0.01 Mo
0.03 Mo
0.05 Mo
0.02 Mo
Bu-8
Bu-9
DDH G3414
most ground below the perv GS contains Py-Qz veins with GS selvages, low Cu & high Mo
DDH11 (11185)
Intense barren quartz veining
DDH1A (11052)
Continental Fault
Klepper Fault
7,000'
5,000'
3,000'
1,000'
SEA LEVEL
Pre-Main Stage
Porphyry Cu-Mo Mineralization
Geology modified from M.H. Reed (1979, 1999)
1
0.5
0
1 km
No vertical exaggeration

Between the Anaconda and Pittsmont domes, and partly overlying the latter, is a large bulb-like mass, or plume, of pervasively sericitized rock (Fig. 1) that is characterized by a stockwork of quartz–pyrite veinlets in which quartz/pyrite ranges from 90:10 to 5:95, and by gray-sericitic alteration selvages (Reed, 1979). These veinlets cut both earlier chalcopyrite- and molybdenite-bearing veinlets, thus constituting yet a third distinct episode of pre-Main Stage alteration and mineralization. This zone of pervasive gray-sericitic alteration grades laterally outward and upward as a halo of moderately to weakly sericitized rock that overlies most of the Anaconda and Pittsmont domes, and that served as the principal loci of Cu–Mo mineralization. Again, crosscutting relationships show that the plume of quartz–pyrite veinlets with associated 'gray-sericitic' alteration is younger than the earliest veinlets of 'early dark mica' and pale green sericitic veinlets and associated K-silicate alteration as well as the somewhat later dark green 'sericite'–chlorite and quartz–molybdenite veinlets, and probably the propylitic assemblages. Only trace amounts of chalcopyrite are present in the 'gray-sericitic' zone, as is consistent with low concentrations of Cu (about 0.05 to 0.20 wt.%) and the near-absence of later large Main Stage veins. Pyrite is the dominant sulfur-bearing mineral. Although sulfate was not observed, cavities common to the quartz–pyrite veinlets may be the vestiges of anhydrite that, because of its retrograde solubility at <375 °C (Holland and Malinin, 1979), was leached by Main Stage fluids.

The younger Main Stage mineralization at Butte produced the famous giant fissure veins that contain the high-grade Cu–Zn–Pb–Ag–Mn ores. These large veins are bordered by an outward succession of alteration halos dominated by "white sericite", followed by kaolinite, and by outermost smectitic forms of "intermediate argillic" alteration (Sales and Meyer, 1948; Meyer and Hemley, 1967; Meyer et al., 1968). In the central part of the district, veinward of the "white" sericitic alteration, is an inner selvage of advanced argillic alteration characterized by such minerals as pyrophyllite, dickite, kaolinite, and local alunite. The Main Stage veins were best developed in the central and western parts of the district, where they were superimposed on most of the early pre-Main Stage porphyry Cu–Mo mineralization in the Anaconda Dome, but only on the upper and western parts of the Pittsmont Dome (Fig. 1). Main Stage veins cut all earlier pre-*Main Stage* veinlets. Main Stage sulfides are dominated by pyrite and exhibit a district-wide zonation (Meyer et al., 1968) from inner high-sulfidation assemblages of chalcocite±covellite in the Central Zone successively outward with decreasing sulfidation state through the Intermediate Zones of bornite and then chalcopyrite plus sphalerite, and the Peripheral Zones of sphalerite plus galena and then an outermost zone dominated by Mn carbonates. In addition, a Deep Level Zone dominated by chalcopyrite underlies the Intermediate Zones. The trace amounts of sulfates that have been reported from Main Stage veins (Meyer et al., 1968) consist of alunite from the Central Zone and barite from all zones. A pervasive smectitic form of "green argillic" alteration after plagioclase is present throughout much of the central and peripheral parts of the district; although the age is uncertain and may be in part Main Stage (Sales and Meyer, 1948), geological and isotopic evidence indicates that the alteration is locally

Fig. 1. (A) Geological map of the central part of the Butte district, simplified from the 1:12,000 map by the Anaconda Company (ca. 1977 by J. Proffett and G. Burns) with compilation and modifications by R. Houston and J. Dilles (Houston, 2001). Bold lines are faults and thin lines are Main Stage base metal veins (Meyer et al., 1968). Porphyry Cu–Mo mineralization is exposed in the Continental pit east of the Continental normal fault, whereas west of the fault, it is at variable depths beneath the surface. Abbreviations: Deep drill holes (DDH), core or mine samples (numbers), and rock symbols from oldest to youngest are Butte Quartz Monzonite (granite) and aplite (BQM), quartz porphyry dikes (Kqp), post-mineral granite porphyry dike (Tgp), Big Butte Complex of the Lowland Creek Volcanics (LCV), rhyolite pyroclastic feeder vent (Tiv), rhyolite pyroclastic wall-vent breccia (Tivb), rhyolite ignimbrite (Ticb), rhyodacite dikes of the LCV (Tird), and Tertiary and Quaternary basin-fill clastic sediments (QTa). The line extending southeastward from the Steward shaft marks the A–A′ cross-section in B. (B) Cross-section illustrating porphyry Cu–Mo sulfide mineralization and wallrock-alteration zones (Reed, 1979, 1999). The magnetite vein zone, with 'early dark mica' and 'pale green sericitic' types of K-silicate alteration, outlines the center of ≈0.4 wt.% Cu mineralization underlying the Anaconda and Pittsmont domes. Molybdenite-bearing veinlets cut the magnetite vein zone, and highest grades of Mo lie at greater depth than those of Cu. The gray-sericitic (GS) alteration zone (plume) is accompanied by quartz–pyrite veinlets that cut the quartz–molybdenite veinlets, which in turn are cut by the Main Stage base-metal veins in the Berkeley Pit and Anaconda Dome.

distinctly younger (Sheppard and Taylor, 1974; Zhang, 2000).

The north-striking and west-dipping Continental Fault passes through the eastern part of the district (Fig. 1). Because this normal fault has as much as 1400 m of vertical displacement, rocks exposed to the east in the area of the Continental Pit represent a deep part of the Pittsmont Dome and, thus, the Butte porphyry Cu–Mo system. Exposures in this area provide the best samples for studies of pre-Main Stage mineralization because, unlike most others in the district, they have been least affected by the later Main Stage hydrothermal fluids.

Temporal details of the late Cretaceous–early Tertiary geological history in the Butte district have been improved by recent geochronological studies (Martin et al., 1999; Snee et al., 1999; Martin and Dilles, 2000; Lund et al., 2002; J.H. Dilles and H. Stein, unpublished data). Important events include emplacement of the host Butte Quartz Monzonite (about 75 Ma), emplacement of quartz porphyry dikes related to pre-Main Stage mineralization (about 66 Ma), pre-Main Stage mineralization (about 66 to 65 Ma), and Main Stage mineralization (about 65 to 62 Ma).

3. Samples, procedures, and conventions

Most samples of drill core and veins examined in this study are identified by a four- or five-digit prefix to indicate that they are archived at Butte in the Geologic Research Laboratory (GRL) collection of the former Anaconda. Samples from the eastern part of the district and most deep drill core are housed by Montana Resources, whereas those from the western part of the district are stored in a building supervised by the Montana Bureau of Mines and Geology. The GRL numbers of the deep diamond-drill holes are given in parentheses as follows: DDH-1 (10969); DDH-1A (11052); DDH-2 (11135); DDH-3 (11148); DDH-5 (11166); DDH-7 (11170); DDH-10 (11172); and DDH-11 (11185).

Sulfur-bearing minerals analyzed in this study are dominated by those formed during pre-Main Stage mineralization. Sampling was purposely selective and directed to drill core and mine localities likely to provide the most information. The minerals were separated either from samples of core from eight deep diamond-drill holes representing a vertical interval of about 2080 m (exclusive of later structural displacement) or from specimens collected from the Steward, Kelly, and other mines (Fig. 1). Sample selection emphasized those containing veinlets bordered either by K-silicate (including ‘early dark mica’, pale green sericitic, and dark green sericitic–chloritic) or by ‘gray-sericitic’ types of alteration. The former provided two or more coexisting or associated (not necessarily contemporaneous) sulfur-bearing minerals, such as anhydrite, chalcopyrite, molybdenite, and (or) pyrite from a single sample, whereas the latter was simply a means of monitoring the isotopic behavior of the single and most ubiquitous sulfide mineral, pyrite. The anhydrite–sulfide veinlets were observed and collected from the Pittsmont Dome only in core from DDH 10 over the interval from 530 to 1294 m. Data are also included for similar anhydrite–pyrite veinlets in samples previously collected from the Steward mine of the Anaconda Dome. Pyrite in quartz veinlets of the ‘gray-sericitic’ assemblage was obtained largely from DDH 1 and its subsurface deflection DDH 1A at depth, which provided a lengthy vertical interval of about 1591 m and a subhorizontal intersection of about 607 m through the central ‘gray-sericitic’ plume and its associated stockwork of veinlets between the Anaconda and Pittsmont domes. We also report analyses for four samples of the relatively rare, late Main Stage, barite–pyrite vein assemblage.

Sulfur-isotope analyses have been performed on 27 sulfate (anhydrite, 23; barite, 4) and 67 sulfide (molybdenite, 6; pyrite, 48; chalcopyrite, 13) mineral concentrates that were extracted by heavy-liquid separation from 47 samples of the deep drill core and 8 ore samples from mine locations. The purity of most mineral concentrates with respect to other sulfur-bearing contaminants was estimated visually and typically exceeded 98%, although some contamination (up to 15%) was encountered with several pyrite–chalcopyrite and molybdenite–chalcopyrite assemblages that were finely crystalline and intimately mixed.

Isotopic analyses were performed on SO_2 gases extracted by conventional methods from the sulfur-bearing minerals. The sulfur in anhydrite was first reduced to H_2S in a boiling solution of hydrochloric–

hydriodic–hypophosphorous acid and was collected as silver sulfide (Thode et al., 1961). Silver sulfide and the other sulfide minerals were mixed with Cu_2O and oxidized under vacuum at 1025 to 1100 °C to SO_2 for isotopic analysis according to methods described by Ohmoto and Rye (1979) and Ohmoto and Goldhaber (1997) (and references therein). Recoveries of sulfur normally exceeded 90 and 95% for sulfate and sulfide minerals, respectively. Isotopic analyses of the SO_2 were performed in the Department of Geological Sciences, University of Missouri-Columbia, and in facilities of the U.S. Geological Survey at the Denver Federal Center, Colorado. The U.S. Geological Survey also provided laboratory and instrumental support for a reconnaissance oxygen-isotope study on a subset of sulfate concentrates (barite, 4; anhydrite, 9) selected from the Butte suite. The $\delta^{18}O$ analyses were performed by mass spectrometry following pyrolysis of the sulfates to CO at 1425 °C by methods modified from Farquhar et al. (1997) using a ThermoFinnigan TC/EA (thermal combustion/elemental analyzer) coupled to a ThermoFinnigan Delta Plus XL mass spectrometer. Also, a trace amount of "magmatic" sulfur from an unaltered sample of Butte Quartz Monzonite was extracted using Kiba reagent (Sasaki et al., 1979; Sakai et al., 1982) and was analyzed for $\delta^{34}S$ at facilities of the Geological Survey of Japan.

The sulfur and oxygen isotope data are presented as conventional per mil values ($\delta^{34}S‰$ and $\delta^{18}O‰$). Those for sulfur are referenced to the meteorite Cañon Diable Troilite (CDT or VCDT) standard and those for oxygen to Standard Mean Ocean Water (SMOW or VSMOW) according to Ohmoto and Goldhaber (1997), Taylor (1997), and Seal et al. (2000). The per mil values may be used to calculate the isotopic separation between two sulfur- or oxygen-bearing compounds (A and B, as minerals, gases, or aqueous species) either from the fractionation factor (α) or from the delta value (Δ) given by

$$\Delta_{A-B} = \delta_A‰ \ \delta_B‰ \approx 1000 \ln \alpha_{A-B} \quad (1)$$

This isotopic separation, or fractionation, is caused by differences in the bond strengths of the isotopes of sulfur or oxygen in different compounds. Because the effect varies inversely with temperature, the fractionation factor (α) or related delta value (Δ) serves as a geothermometer provided it has been previously determined over a range of temperatures for the appropriate compounds, preferably by experiment or less reliably from theory or empirical relationships.

The total analytical error based on replicated extractions and isotopic analyses of selected samples and a laboratory standard (Bingham pyrite) is less than 0.2‰ for sulfide–sulfur, about 0.3‰ for sulfate–sulfur, and about 0.3‰ for sulfate-oxygen. The isotopic data for concentrates contaminated by another sulfide have been adjusted by means of algebraic equations using the raw analytical data and percentage estimates of mineral contamination as visually inferred.

4. Previous sulfur-isotope investigations

The first isotopic analyses of sulfur in sulfides from the Butte district were reported by Jensen (1959) as part of a reconnaissance investigation of hydrothermal and magmatic sulfides from largely North American localities. He noted that, unlike the broad isotopic variability for many of these deposits, 19 sulfide concentrates from Main Stage mineralization at Butte exhibited a relatively narrow range of $\delta^{34}S$ values near 0‰. This isotopic homogeneity was consistent with a single reservoir or common source for Main Stage hydrothermal fluids, as originally proposed by Sales (1914) on the basis of geological inferences. Ames (1962) re-analyzed a number of these samples using improved laboratory procedures and detected a weak apparent gradient of increasing $\delta^{34}S$ values possibly related to thermal metamorphism of Main Stage sulfides as described by Sales and Meyer (1951) in Butte Quartz Monzonite immediately adjacent to post-ore rhyolite dikes. Field (1966) contributed two additional analyses for Main Stage sulfides from the Berkeley Pit at Butte.

Lange and Cheney (1971) performed an extensive district-wide sulfur isotopic investigation of Butte based on 123 concentrates of different sulfide minerals extracted from samples of the Deep Level, Central, Intermediate, and Peripheral zones. Although most were representative of Main Stage mineralization, one pyrite and four molybdenite concentrates belonged to the earlier pre-Main Stage. Significant among the conclusions was the documentation of primary fractionation between different sulfide min-

erals; the theoretical concept had been initially proposed by Sakai (1968) and was subsequently considered more fully by Bachinski (1969) using a wider array of mineral thermochemical data and, in part, the Butte isotopic data of Jensen (1959) and Ames (1962). Lange and Cheney (1971) also noted isotopic similarity between sulfides of the east–west-striking Anaconda and northwest-striking Blue vein systems that was consistent with the geological evidence supporting near-contemporaneity and mutually crosscutting relations of these two Main Stage vein sets (cf. Proffett, 1973) and the previously inferred isotopic homogeneity of the Butte hydrothermal system. An outward increase in the $\delta^{34}S$ values of the sulfides, especially pyrite, was ascribed to increasing pH rather than to decreasing temperature as the fluids moved upward and outward from the Central Zone. With these data, the range of $\delta^{34}S$ values for 144 sulfide concentrates from the Butte district was increased slightly from −3.7‰ to 4.8‰, with a mean of about 0.4‰.

In a preliminary sulfur isotopic survey of sulfate–sulfide mineral assemblages in porphyry-type deposits, Field et al. (1983) included three samples of pre-Main Stage anhydrite–pyrite veinlets from the 4200 level of the Steward mine at Butte. The anhydrite was appreciably enriched in $\delta^{34}S$ (14.1‰ to 18.2‰) relative to coexisting pyrite (2.7‰ to 3.0‰), as is consistent with fractionation theory, and the mineral pairs provided reasonable isotopic temperatures approximating the range of 400 to 500 °C.

Lange and Krouse (1984) undertook a detailed isotopic study of 69 sulfide concentrates of mostly pyrite collected from a restricted area of a single N–W vein and adjacent wallrock within the Intermediate Zone on the 3200 level of the Steward mine. Although the $\delta^{34}S$ values of all sulfides were within the previously established range for the district, those for 58 concentrates of vein, veinlet, and disseminated textural forms of pyrite exhibited a particularly narrow spread from 1.3‰ to 3.9‰. Within this narrow range, however, pyrite disseminated in wallrock was slightly depleted in ^{34}S relative to nearby vein pyrite, and this depletion apparently was progressive with increasing distance from the vein. Although fractionation effects related to diffusion or changing pH–Eh conditions of the hydrothermal fluid were considered to account for the observed isotopic gradients, the mechanism favored by Lange and Krouse (1984) was that of mixing through the overprinting of relatively ^{34}S-enriched Main Stage vein mineralization on an earlier and relatively ^{34}S-depleted pre-Main Stage disseminated mineralization.

5. New sulfur and oxygen isotopic data

Our work, as previously noted, is concerned almost exclusively with pre-Main Stage mineralization. A single analysis of whole-rock "magmatic" sulfur in a sample of unaltered Butte Quartz Monzonite provided a $\delta^{34}S$ value of −0.4‰. As discussed below, the mineralogical source of the sulfur is uncertain because of the small concentration (14 g tonne^{-1} S=14 ppm S) in the sample. The remainder of our data are based on sulfur-bearing mineral concentrates separated from samples collected from deep drill core and the various mines as shown in Fig. 1. Particular emphasis was given to the sulfur-bearing minerals in veinlets or disseminations that accompany pre-Main Stage K-silicate and gray-sericitic types of alteration. Quartz veinlets with or without molybdenite, pyrite, or chalcopyrite and associated with K-silicate alteration were obtained from holes DDH 2 and 10 into the Pittsmont Dome, and from samples from the Kelly and Steward mines in the Anaconda Dome (Fig. 1). Anhydrite, commonly with sulfides, was found only in DDH 10 and in four samples from the Steward mine. Samples of pyrite in pre-Main Stage quartz veinlets having gray-sericitic selvages were collected from DDH 1, 1A, 3, 5, 7, and 11. Because the zones of K-silicate and gray-sericitic types of alteration and mineralization in DDH 10 and DDH 1/1A, respectively, are intense, pervasive, and vertically extensive (thousands of meters), core from these holes was sampled at multiple locations. In addition, analyses of four barite–pyrite pairs from late Main Stage vein mineralization were undertaken for purposes of comparison. Finally, a reconnaissance $\delta^{18}O$ study was undertaken on a subset of 13 sulfate samples to examine anomalous $\delta^{34}S$ relationships among the samples of pre-Main Stage anhydrite of the Pittsmont and Anaconda domes, and between the anhydrite and the late Main Stage barite.

Sample numbers, locations, brief descriptions, and $\delta^{34}S$ values are recorded in Table 1 for sulfate and sulfide minerals of the pre-Main Stage K-silicate alteration, later Main Stage hydrothermal events, and the "magmatic" stage. Similar data are listed in Table 2 for pyrite in late pre-Main Stage quartz veinlets defined by gray-sericitic alteration selvages. The tabulated $\delta^{34}S$ data for pre-Main Stage sulfates and sulfides of the K-

Table 1
Sulfur-isotope data for sulfate and sulfide minerals of late Main Stage veins, pre-Main Stage K-silicate assemblages, and of possible "magmatic" sulfur at Butte

Sample no.	Mine/DDH	Vein mineralization	Alteration, selvage/host	$\delta^{34}S$ (‰, CDT)				
				Brt	Anh	Mo	Py	Ccp
Main Stage veins								
MMM2236M	Buffalo; 500L	Qtz–Py–Cv–Brt	Qtz–Ser	27.3			1.3	
DUDAS 3	Mountain Con	Brt–Py–Qtz–Cc	probably Qtz–Ser	18.6			2.2	
GRL 9274	Steward; 4000L	Py–Brt–Ccp	probably Qtz–Ser	13.5			2.3	
GRL 3183	Leonard; 3400L	Py–Brt–Qtz–Gn	probably Qtz–Ser	4.4			1.3	
Pre-Main Stage, Anaconda Dome								
10759-336	Kelly; 2000L	diss Py, Ccp	DGS; host KSi				0.6	1.0
10854-643	Kelly; 2000L	Qtz–Py–Ser–Chl	DGS; host KSi				0.4	
10772-31	Kelly, 3400L	diss Py, Ccp	PGS; host KSi				1.7	0.5
10778-4	Steward; 3400L	Qtz–Ser–Py–Ccp	PGS; host KSi				1.9	–0.1
Bu-8a	Steward; 4200L	Anh–Py	PGS; host KSi		18.2		3.0	
Bu-8b	Steward; 4200L	Anh–Py	PGS; host KSi		18.1		2.3	
Bu-9a	Steward; 4200L	Qtz–Anh–Py	EDM; host KSi		14.7		2.9	
Bu-9b	Steward; 4200L	Qtz–Anh–Py	EDM; host KSi		14.1		2.7	
Pre-Main Stage, Pittsmont Dome								
11172-1743	Continental DDH 10	Qtz–Anh	EDM; host KSi		11.6			
11172-2262.5	Continental	Qtz–Py–Anh	PGS; host KSi		11.2		3.4	
11172-2264.5	Continental	Py–Qtz–Anh	PGS; host KSi		12.2		2.8	
11172-2276.5	Continental	Qtz–Anh–Py	EDM; host KSi		11.9		3.4	
11172-2424.4	Continental	Anh–Qtz–Py	PGS; Aplite host KSi		12.3		2.4	
11172-2460.5	Continental	Qtz–Anh–(Py)	weak Qtz–Ser; host KSi		9.8		0.5	
11172-2749	Continental	Qtz–Anh–Mo	PGS; Bt Bx host KSi		12.1	4.1		
11172-2948	Continental	Qtz–Anh–Mo	PGS; host KSi		12.5	4.0		
11172-3158	Continental	Qtz–Anh–Ccp–Mo	EDM; host KSi		12.7	4.7		2.0
11172-3252.5	Continental	Anh–Qtz–Py	PGS; host KSi		12.3		2.9	
11172-3429.5	Continental	Qtz–Kfs–Anh–Ccp	EDM; host KSi		12.7			0.7
11172-3505.5	Continental	Kfs–Qtz–Anh	PGS; host KSi		12.9			
11172-3871	Continental	Qtz–Anh–Py–Mo	EDM; host KSi		12.3	4.4	3.4	
11172-3874	Continental	Qtz–Anh–Py–Ccp–Mag	EDM; host KSi		12.7		3.4	2.3
11172-3886.5	Continental	Qtz–Anh–Ccp–Mo	EDM; host KSi		12.6	3.0		1.6
11172-3907.5	Continental	Qtz–Anh–Py–Ccp	EDM; host KSi; late PGS		12.8		2.9	1.5
11172-3920	Continental	Qtz–Anh–Ccp–Mag	EDM; host KSi		11.8			1.3
11172-4208	Continental	Qtz–Anh–Ccp	EDM; host KSi; late PGS		12.6			2.3
11172-4245	Continental	Qtz–Anh–Mo–Ccp	EDM; host KSi; late PGS?		12.6	4.1		3.0
11135-3481	W. Continental DDH 2	Qtz–Py–Ccp	EDM; host KSi; late argillic				3.1	2.1
11135-3586	W. Continental	Qtz–Py–Ccp	Bt Bx; host KSi; late argillic				1.6	0.4
"*Magmatic*" *sulfur*								
Bd-1	Butte Qtz Monz.	unmineralized	BQM, unaltered; 14 ppm S				–0.4	

Anh, anhydrite; BQM, Butte Quartz Monzonite; Brt, barite; Bt, biotite; Bx, breccia; Cc, chalcocite; Ccp, chalcopyrite; Chl, chlorite; Cv, covellite; diss, disseminated; DGS, dark green sericitic; EDM, early dark micaceous; Gn, galena; Kfs, K-feldspar; KSi, K-silicate assemblage; Mag, magnetite; Mo, molybdenite; PGS, pale green sericitic; Py, pyrite; Otz: quartz; Ser, sericite.

Table 2
Sulfur-isotope data for pyrite in quartz–pyrite veinlets from samples of the pre-Main Stage gray-sericitic (GS) assemblage at Butte

Sample	Description	δ^{34}S (‰, CDT)
10969–1227 (DDH-1)	Qtz–Py (60:40) veinlet with successive 1 cm GS envelopes and with remnant biotite and white clay in host.	2.7
10969-2251	Py–Qtz veinlets with trace relict Mo in GS altered host and white clay in feldspars.	2.3
10969-2627	Py–Qtz (80:20) veinlet with trace Ccp and GS selvage to host.	2.3
11052-2851 (DDH-1A)	Py–Qtz veinlet with GS selvage cut by barren Qtz and Qtz–Py–Mo veinlets with 4 mm selvage.	2.7
10969-5452 (DDH-1)	Py–Qtz veinlet with minor hematite and GS selvage.	2.4
10969-5618	Vuggy Py–Qtz veinlet with remnant biotite and PGS in GS selvage.	2.2
10969-6448	Barren Qtz veinlets cut by Qtz–Py veinlets with GS selvages.	2.4
11052-5532 (DDH-1A)	Vuggy Qtz–Py veinlet with host altered to grayish PGS.	3.4
11052-6639	Barren Qtz and vuggy Py–Qtz veinlets with grayish PGS host.	2.0
11052-7037	Barren Qtz and vuggy Py–Qtz veinlets with fragment (?) of vuggy Qtz–Mo–Py veinlet in grayish PGS altered host.	2.8
11052-7083	Barren Qtz veinlet with minor Py associated with apparent Main Stage argillic alteration and mineralization.	4.3
11052-7285	Barren Qtz and Py–Qtz veinlets with grayish PGS alteration.	2.6
11052-7369	Pre-Main Stage Qtz–Mo veinlet reopened by later Py–Qtz veinlet with GS and PGS alteration selvages on the host.	3.8
11052-7522	Barren Qtz veinlets in aplite cut by late vuggy Py–Qtz veinlets.	2.6
11148-888 (DDH-3)	Py–Qtz (90:10) veinlet with 3 cm GS selvage, some remnant biotite and weak argillic alteration.	3.0
11148-1140	Py–Qtz veinlet with GS and remnant biotite in selvage.	2.7
11166-5885.5 (DDH-5)	Early vuggy Qtz–Py–Mo veinlet cut by vuggy Qtz–Py veinlet with sericitic alteration.	2.9
11170-864.5 (DDH-7)	Vuggy Py–Qtz (90:10) veinlet with GS and weak argillic selvages.	3.5
11170-1767	Py–Qtz (70:30) veinlet with GS alteration.	2.8
11170-1790	Py–Qtz veinlets with GS alteration.	3.7
11170-2423	Py–Qtz (75:25) veinlet with GS alteration.	2.1
11170-4871.5	Late Py–Qtz (90:10) veinlet with 2 cm GS selvage.	2.2
11170-4936	Vuggy Qtz–Py (70:30) veinlet with GS and PGS selvages cutting Qtz–Mo veinlet.	1.7
11170-5333	Vuggy Py–Qtz–hematite veinlet with 6 mm GS selvage with remnant biotite.	1.9
11185-1595 (DDH-11)	Qtz–Py (10:90) veinlet with GS selvage containing remnant biotite and cut by Main Stage Qtz–Py veinlets with trace bornite and enargite.	3.1
	N=25 Mean=2.7‰	
	Range=1.7‰ to 4.3‰ S.D.=±0.64‰	

Abbreviations as in Table 1.

silicate assemblage are summarized in Fig. 2. This work has provided a database for Butte hydrothermal sulfates: 23 values of δ^{34}S for pre-Main Stage anhydrite that range from 9.8‰ to 18.2‰ (mean 12.9‰), all of which are significantly enriched in ^{34}S relative to their associated sulfides (0.5‰ to 4.7‰; Table 1). Nonetheless, the four samples of anhydrite from the Anaconda Dome (ranging from 14.1‰ to 18.2‰) display moderately higher ^{34}S enrichment and a slightly larger range than do their 19 counterparts from the Pittsmont Dome (between 9.8‰ and 12.9‰, but with 18 values from 11.2‰ to 12.9‰). The δ^{34}S values of four samples of late Main Stage barite exhibit an unusually broad range from 4.4‰ to 27.3‰, whereas the associated pyrite has a narrow range (1.3‰ to 2.3‰) of typical sulfide compositions. The 38 sulfide concentrates representative of the K-silicate assemblages from the Pittsmont and Anaconda domes exhibit a relatively narrow range of δ^{34}S values (from −0.1‰ to 4.7‰; Table 1; Fig. 2). However, the ranges for individual sulfide–mineral species are more restricted: molybdenite (6, from 3.0‰ to 4.7‰); pyrite (19, from 0.4 to 3.4‰); and chalcopyrite (13, −0.1‰ to 3.0‰). The data reported by Lange and Cheney (1971) for one pyrite and four molybdenite concentrates (pyrite, 1.7‰, and molybdenite, 2.6‰ to 3.4‰) of the pre-Main Stage are within or near these ranges. Pyrite is abundantly and almost exclusively the only

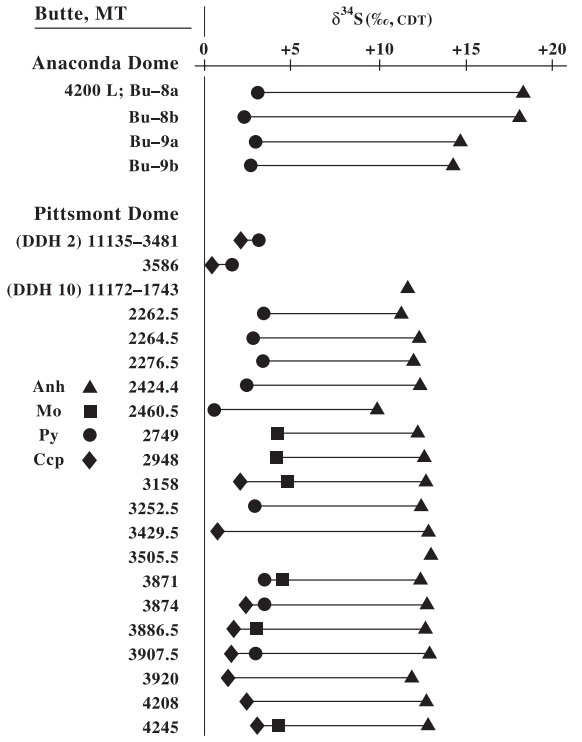

Fig. 2. Summary of the sulfur-isotope data for anhydrite (Anh) and associated sulfides in pre-Main Stage veinlets of the K-silicate assemblage of the Anaconda and Pittsmont Domes. Mo=molybdenite, Py=pyrite, Ccp=chalcopyrite.

sulfide and sulfur-bearing mineral in the pre-Main Stage gray-sericitic assemblage, which is best developed in the large hydrothermal plume between the Pittsmont and Anaconda domes (Fig. 1). The $\delta^{34}S$ values for 25 pyrite concentrates taken from samples of drill core (DDH 1, 1A, 7) from within this plume and from its eastern flank (DDH 3, 5, 11) are listed in Table 2. The values from this suite range narrowly from 1.7‰ to 4.3‰ and do not warrant a graphical portrayal. However, they do overlap and extend the ^{34}S-enriched end of the range for pyrite (0.5‰ to 3.4‰) of the K-silicate assemblage.

The database for Butte sulfides now consists of 281 analyses that range from −3.7‰ to 4.8‰, unchanged from the earlier study by Lange and Cheney (1971). However, the mean value has increased from about 0.4‰ to 1.4‰ because of the preponderance of relatively ^{34}S-enriched analyses for pyrite and other sulfides reported by Lange and Krouse (1984) and by this investigation. A summary (not illustrated) of all $\delta^{34}S$ analyses for minerals of the Butte district shows at least two obvious trends: (1) all sulfates, with a single exception, are significantly enriched in $\delta^{34}S$ relative to sulfides, and (2) molybdenite exhibits a subtle ^{34}S enrichment with respect to pyrite, as do these two sulfides largely with respect to all others. Main Stage sulfides are mostly narrowly and symmetrically distributed around 0‰, whereas those of the pre-Main Stage are slightly and almost entirely enriched in ^{34}S, but this apparent trend is probably an artifact of fractionation related to the lower temperatures and more diverse sulfide mineralogy of the Main Stage hydrothermal suite.

6. Discussion

The sections that follow consider isotopic equilibrium and temperature estimates determined from sulfate–sulfide and sulfide–sulfide mineral pairs, the compositions of total sulfur ($\delta^{34}S_{\Sigma S}$) and sulfate/sulfide ratios expressed as sulfate mole fractions ($X_{SO_4^{2-}}$) in the various Butte hydrothermal systems, the possible causes of sulfur isotopic differences among samples of pre-Main Stage anhydrite of the Pittsmont and Anaconda domes and unusually broad isotopic variations among late Main Stage barite, and the results of an $\delta^{18}O$ study for a subset of these sulfates.

6.1. Isotopic equilibrium and temperature estimates

The $\delta^{34}S$ values of the anhydrite are invariably heavier than those of associated or coexisting sulfides (Table 1; Fig. 2), and although the ranges of these values overlap the groups of specific sulfide minerals, without exception in samples that contain sulfide–mineral pairs, molybdenite is enriched in ^{34}S relative to pyrite, and pyrite in turn is similarly enriched in ^{34}S relative to chalcopyrite. In addition, two of three samples representing pre-Main Stage sericitic subtypes (pale green sericitic and dark green sericitic–chloritic) of the K-silicate assemblage also contain ^{34}S-enriched pyrite relative to associated chalcopyrite. These isotopic trends have been observed elsewhere, including at other porphyry Cu–Mo deposits, and the trends are consistent with isotope equilibrium theory and sulfur-isotope fractionation trends determined

from theoretical, experimental, and empirical relationships (Ohmoto and Rye, 1979; Ohmoto and Lasaga, 1982; Ohmoto and Goldhaber, 1997, and references therein). These investigations have documented that sulfates are most enriched in ^{34}S and that progressive ^{34}S depletion follows in the order molybdenite, pyrite, sphalerite, chalcopyrite, bornite, covellite, galena, and chalcocite (Ohmoto and Rye, 1979).

If the isotopic differences between the Butte sulfates and sulfides represent the effects of primary equilibrium isotopic exchange reactions at the time of mineral deposition, then isotopic temperature estimates may be determined from delta values for the various mineral pairs as calculated from the $\delta^{34}S‰$ data of Table 1 using Eq. (1). The Δ values are then entered into fractionation equations for the appropriate mineral pairs to obtain the temperature estimates. Fractionation equations for sulfate–H_2S and sulfide–H_2S isotopic equilibria given by Ohmoto and Lasaga (1982) and Ohmoto and Rye (1979), respectively, were combined to calculate temperature estimates for the various sulfate–sulfide mineral pairs contained in samples of the K-silicate assemblage from the Anaconda and Pittsmont domes. The results are listed in Table 3 for anhydrite–molybdenite (6), anhydrite–pyrite (13), and anhydrite–chalcopyrite (8) mineral pairs. Delta values for the 27 sulfate–sulfide pairs range from 7.8 to 15.8, and those for the 23 mineral pairs of the Pittsmont Dome range from 7.8 to 12.0. Although the range of calculated temperatures for the Pittsmont Dome is from 480 to 640 °C, the range within a specific mineral-pair group approximates 100 °C or less. The consistency in temperatures provided by two mineral pairs from the same sample is moderately good, but it is clear from such comparisons, and the means and ranges, that the anhydrite–

Table 3
Sulfur isotopic temperature estimates for sulfate–sulfide mineral pairs of the pre-Main Stage K-silicate assemblage at Butte

	$\Delta_{Anh–Mo}$	T, °C	$\Delta_{Anh–Py}$	T, °C	$\Delta_{Anh–Ccp}$	T, °C
Anaconda Dome (Steward Mine)						
Bu-8a (4200 L)			15.2	370		
Bu-8b (4200 L)			15.8	360		
Bu-9a (4200 L)			11.8	460		
Bu-9b (4200 L)			11.4	475		
Mean			13.6 (4)	415		
Range			11.4–15.8	360–475		
Pittsmont Dome (DDH 10)						
2262.5			7.8	640		
2264.5			9.4	555		
2276.5			8.5	605		
2424.4			9.9	535		
2460.5			9.3	560		
2749.0	8.0	625				
2948.0	8.5	595				
3158.0	8.0	625			10.7	530
3252.5			9.4	555		
3429.5					12.0	480
3871.0	7.9	630	8.9	580		
3874.0			9.3	560	10.4	540
3886.5	9.6	545			11.0	515
3907.5			9.9	535	11.3	505
3920.0					10.5	535
4208.0					10.3	545
4245.0	8.5	595			9.6	575
Mean	8.4 (6)	605	9.2 (9)	570	10.7 (8)	530
Range	7.9–9.6	545–630	7.8–9.9	535–640	9.6–12.0	480–575

Temperatures calculated from delta values using the fractionation equations of Ohmoto and Rye (1979) and Ohmoto and Lasaga (1982). Anaconda Dome samples are from the Stewart mine, and Pittsmont Dome samples are from DDH 10.

molybdenite pairs invariably provide the highest temperatures and the anhydrite–chalcopyrite pairs provide the lowest. The reason for such consistent temperature differences between different mineral pairs, and yet among largely coexisting minerals, is uncertain. Possible explanations include: (1) subtle paragenetic differences in mineral deposition; (2) systematic analytical errors; (3) small errors in the fractionation equations for sulfide–H_2S equilibria; and (4) isotopic disequilibrium and (or) retrograde effects. Low temperatures derived from pyrite–chalcopyrite fractionations, to be described, suggest that chalcopyrite has undergone retrograde reactions. Regardless of potential shortcomings, the isotopic temperature estimates (mostly from 500 to 630 °C) obtained from the three anhydrite–sulfide mineral-pair systems are in reasonable agreement with 'early dark mica' and K-silicate petrology (Roberts, 1975; Brimhall, 1977), and with fluid-inclusion homogenization temperatures that range from 350 to 390 °C (Roberts, 1975) and from 320 to 390 °C (Rusk et al., 1999, 2000, 2002; Rusk, 2003) if a pressure correction of about 1.7 kbar is applied to account for depth at the time of porphyry-type pre-Main Stage K-silicate alteration and mineralization.

Delta values for four anhydrite–pyrite pairs from the Anaconda Dome (Table 3) are 11.4‰ to 15.8‰, which are higher than those for equivalent mineral pairs from the Pittsmont Dome (7.8‰ to 9.9‰), and the calculated temperatures are proportionately lower (360 to 475 °C). There are at least three possible explanations for this apparent temperature difference. First, samples collected from the 4200 level of the Steward mine in the Anaconda Dome are topographically equivalent to those of core from the 1237 m depth interval of DDH-10 (~573 m above sea level) in the Pittsmont Dome (Fig. 1). However, restoration of vertical post-mineralization displacement of as much as 1370 m by the Continental Fault places the entire sulfate–sulfide core sample interval (531 to 1294 m) from DDH-10 at between −91 and −854 m below sea level relative to the Anaconda Dome (at its present position). Thus, the Pittsmont Dome samples were originally structurally much deeper than those of the Anaconda Dome, which might favor higher temperatures in the former. Second, all samples collected from the Anaconda and Pittsmont domes are intimately associated with veinlets of 'early dark mica' and the K-silicate alteration assemblage. However, the anhydrite–pyrite veinlets from samples Bu-8a and 8b of the Anaconda Dome (Table 1) are distinguished by having a K-feldspar-stable selvage of quartz–'sericite' between the veinlet and the K-silicate-altered Butte Quartz Monzonite host. This sericitic alteration represents a lower temperature assemblage than does the K-silicate, and it may not be fortuitous that the anhydrite–pyrite pairs from these samples provide the lowest temperatures (360 to 370 °C, Table 3) of any from the suite. However, the relationship of these thin (<2 cm) alteration selvages to either the pre-Main Stage 'gray-sericitic' plume or to the later Main Stage white sericitic alteration is unknown, although both are nearby. Nonetheless, the widespread presence of Main Stage veinlets in the Anaconda Dome area supports the possibility of retrograde overprinting to account for the relatively ^{34}S-enriched anhydrite and lower isotopic temperatures. Yet, a third possible interpretation, discussed in a later section, is that isotopic equilibrium between SO_4^{2-} and H_2S was lacking because of brine–vapor unmixing in the samples from the Anaconda Dome.

The previously noted progressive, relative depletion of ^{34}S in the sulfide sequence from molybdenite through pyrite to chalcopyrite (Table 1; Fig. 2) suggests a close approach to equilibrium between the different sulfide minerals. Assuming equilibrium, these sulfide–sulfide mineral pairs might provide additional isotopic temperature estimates and offer insight into reason(s) for the consistently decreasing mean temperatures calculated from the anhydrite–molybdenite, anhydrite–pyrite, and anhydrite–chalcopyrite mineral pairs, respectively. Because the sulfide–sulfide pairs from the K-silicate sample suite are relatively few in number (11) and provided some unexpected results, relevant data from previous Main Stage studies yield 10 additional sulfide–sulfide pairs for minerals equivalent to those of the pre-Main Stage suite.

Calculated sulfide–sulfide temperatures are highly variable (−175 to 950 °C) and mostly lower than those obtained from sulfate–sulfide equilibria (Table 3). All four molybdenite–pyrite pairs give unrealistically low temperatures of −175 to −50 °C. Four of 14 pyrite–chalcopyrite pairs represent disequilibrium or impossibly high temperatures of 675 to 950 °C, whereas the 10 remaining pairs provide unreasonably

low temperatures (150 to 400 °C), as do three molybdenite–chalcopyrite pairs (155 to 400 °C). Possible causes of apparent disequilibrium and unreasonable temperatures among these sulfide pairs may be lack of contemporaneity, retrograde effects, or problems with the fractionation equation for one or both of the minerals. Pyrite has a broad zonal and paragenetic distribution throughout the Butte district, and many or most veinlets with both molybdenite and pyrite have been refractured and mineralized by later quartz–pyrite of the pre-Main Stage gray-sericitic or Main Stage hydrothermal events. In addition, the molybdenite–pyrite fractionation equation is probably inexact because it has been derived only partly by experimentation (Ohmoto and Rye, 1979). Moreover, the A factor of this equation (Ohmoto and Rye, 1979; Ohmoto and Goldhaber, 1997) is exceedingly small (0.05) in contrast to most other common sulfur-bearing mineral-pair systems (such as molybdenite–chalcopyrite, 0.5; anhydrite–molybdenite, 6.01); thus, calculated temperatures may also be strongly perturbed by analytical errors. Moreover, and as previously noted, the lack of contemporaneity for molybdenite and pyrite may be a source of error. The relatively lower temperatures commonly recorded by chalcopyrite when paired with anhydrite (Table 3) or pyrite (Table 4) may likely relate to its propensity to reequilibrate rapidly (<1 day) at low temperature (<300 °C) and yield chemical compositions that reflect temperatures of <200 to 300 °C according to Barton and Skinner (1979). Therefore, the isotopic composition of chalcopyrite may be expected to re-equilibrate in response to changes in temperature, an inference that is supported by the decrease in strength of metal–sulfur bonds in the order molybdenite, pyrite, sphalerite, chalcopyrite (Sakai, 1968; Bachinski, 1969; Ohmoto and Rye, 1979). Thus, with decreasing temperature in hydrothermal systems the sulfides least likely to reequilibrate would be molybdenite and pyrite, and those increasingly likely would

Table 4
Means and ranges of $\delta^{34}S$ per mil values for selected and (or) widespread sulfate and sulfide minerals of the Butte District and the calculated values of coexisting H_2S

Mineral assemblage/zone		N	$\delta^{34}S$ (‰, CDT)$_{Mineral}$		$\delta^{34}S$ (‰, CDT)$_{H_2S}$		T, °C
			Mean	Range	Mean	Range	
Sphalerite	PZ	6	0.5	−2.0 to 3.2	0.2	−2.3 to 2.9	275
	IZ	5	0.6	0.4 to 0.9	0.3	0.1 to 0.6	275
Chalcopyrite	IZ	6	0.8	−1.0 to 3.1	1.0	−0.8 to 3.3	275
	CZ	1	0		0.2		300
	DLZ	3	−0.9	−2.2 to −0.1	−0.7	−2.0 to 0.1	300
	DGS-A	3	0.5	−0.1 to 1.0	0.6	0 to 1.1	450
	KSi-P	10	1.7	0.4 to 3.0	1.8	0.5 to 3.1	600
Pyrite	PZ	8	2.7	1.3 to 4.8	1.4	0 to 3.5	275
	IZ	86	2.4	−0.9 to 3.9	1.1	−2.2 to 2.6	275
	CZ	20	0.9	−1.8 to 3.6	−0.3	−3.0 to 2.4	300
	DLZ	17	1.0	−0.1 to 2.7	−0.2	−1.3 to 1.5	300
	PGS-A	4	1.1	0.4 to 1.9	0.3	−0.4 to 1.1	400
	GS	25	2.7	1.7 to 4.3	1.8	0.8 to 3.4	400
	KSi-P	15	2.7	0.5 to 3.4	2.2	0 to 2.9	600
Molybdenite	KSi	10	3.6	2.6 to 4.7	3.0	2.0 to 4.1	600
Barite	PZ	1	27.3		0.7		215
Anhydrite	KSi-A	4	16.3	14.1 to 18.2	3.4	1.2 to 5.3	450
	KSi-P	19	12.2	9.8 to 12.9	3.2	0.8 to 3.9	600
"Magmatic"	Sulfur	1	−0.4		≅0?		800

The calculated values for coexisting H_2S at assumed temperatures based on the fractionation equations of Ohmoto and Rye (1979) and Ohmoto and Lasaga (1982). Sulfur isotope data for Main Stage sulfides listed by zones (CZ, DLZ, IZ, and PZ) as defined by Meyer et al. (1968) are from Jensen (1959), Ames (1962), Lange and Cheney (1971), and Lange and Krouse (1984). The data are listed by mineral and by alteration assemblage or mineral–metal zone, generally from shallow (lower temperature) to deep (higher temperature) as implied by Table 1 and proposed by Meyer et al. (1968). Suffixes A and P refer to the Anaconda and Pittsmont Domes, respectively. See text for basis of assumed temperatures.

be sphalerite, chalcopyrite, bornite, galena, and chalcocite.

6.2. Isotopic composition of total sulfur in the Butte magmatic–hydrothermal systems

Knowledge of the isotopic composition of total sulfur ($\delta^{34}S_{\Sigma S}$) in deposits composed of sulfide and (or) sulfate minerals may, with geological input, provide insight as to the provenance of sulfur and the conditions of mineral formation. However, and contrary to the assumptions of many previous investigators, the pioneering studies of Sakai (1968) and Ohmoto (1972) demonstrated that the $\delta^{34}S$ values for a suite of sulfide, or sulfate, minerals cannot of themselves be diagnostic of the overall isotopic composition of a particular mineral deposit. The reason for this assertion is that in any system containing both oxidized (SO_4^{2-} or SO_2) and reduced (H_2S) species of sulfur, the isotopic compositions of either sulfate or sulfide minerals formed therein are dependent not only on the temperature and $\delta^{34}S_{\Sigma S}$ of the system, but also on the ratio of oxidized to reduced sulfur species. Moreover, this ratio is also controlled by the acidity (pH) and oxidation state (fO_2) of the system, which affect the kinds and proportions of the oxidized and reduced sulfur species (Ohmoto, 1972). The presence of sulfate (anhydrite) with sulfides (molybdenite, pyrite, and chalcopyrite) in quartz veinlets of the K-silicate assemblage provides a means of approximating the $\delta^{34}S_{\Sigma S}$ value for the pre-Main Stage hydrothermal system of the Pittsmont Dome. Although fractionation theory suggests that the $\delta^{34}S_{\Sigma S}$ value for this deposit must fall between that of the ^{34}S-enriched anhydrite (mean 12.2‰) and that of the relatively ^{34}S-depleted sulfides (mean 2.6‰), as listed in Table 1, a more precise approximation requires an estimate of oxidized to reduced sulfur. The following sections discuss several approaches taken to assess the values of $\delta^{34}S_{\Sigma S}$ and the proportions of oxidized to reduced sulfur in the Butte hydrothermal systems.

6.2.1. Composition of possible "magmatic" sulfur in the Butte Quartz Monzonite

A single sample of unaltered and unmineralized Butte Quartz Monzonite (Bd-1, Table 1) collected about 8 km southeast of the Butte deposits gave an isotopic value of −0.4‰. The sulfur is presumed to be of magmatic origin, but the mineralogical source is unknown. It may be either sulfate–sulfur as a trace to minor constituent of apatite as described by Streck and Dilles (1998) and by Sha and Chappell (1999) for granitic rocks of Nevada and Australia, respectively, or sulfide–sulfur that is dispersed at low concentrations as tiny magmatic sulfides in most continental and oceanic igneous rocks (Newhouse, 1936; Sakai et al., 1982; Field et al., 1984; Borrok et al., 1999). The isotopic value of −0.4‰ suggests a sulfide source, and falls within the range (0±3‰) for most magmatic sulfide values (Ohmoto and Rye, 1979). A sulfide source is entirely consistent with the results of petrographic studies by Brownlow and Kurz (1979), who observed small, but variable amounts of disseminated sulfides averaging ≈100 to 200 g tonne^{-1} S in unaltered phases of the Boulder batholith. The predominant sulfide is pyrite, although chalcopyrite and pyrrhotite or mackinawite may be present as inclusions within pyrite and within or along the grain boundaries of oxide and silicate minerals of the host.

The Butte Quartz Monzonite contains the assemblage titanite+magnetite+quartz, which requires strongly oxidized conditions (oxygen fugacity> NNO+2 log units at 700–800 °C and 200 MPa water pressure; Dilles, 1987; Wones, 1989) under which SO_4^{2-} would predominate over H_2S as the melt sulfur-species (cf. Ohmoto and Rye, 1979; Kiyosu and Kurahashi, 1983; Whitney, 1984; Ohmoto, 1986; Burnham, 1997). Thus, if the bulk analysis of −0.4‰ records sulfate–sulfur in apatite, this value may be representative of bulk sulfur in the Butte Quartz Monzonite. However, if this value represents sulfide–sulfur in the rock, then the calculated composition of sulfate in the melt (at 700 °C, using $\Delta_{sulfate-sulfide}$=7.4‰, from Ohmoto and Lasaga, 1982) would be ~7‰, which would approximate the composition of the magmatic sulfur reservoir. All values between −0.4‰ and 7‰ are also possible for a bulk rock with mixtures of sulfide– and sulfate–sulfur. Because the mineralized quartz porphyry dikes are about 8 m.y. younger than Butte Quartz Monzonite, the latter's sulfur isotopic composition may not be directly relevant to the ores. However, it is notable that the Butte Quartz Monzonite likely has a sulfur isotopic composition greater than ~3‰, which suggests incorportation of isotopically

heavy crustal sulfur, similar to that required for the pre-Main Stage ores described below.

6.2.2. Sulfur species in magmatic gases and resultant hydrothermal fluids

For magmas such as the Butte quartz porphyry in which SO_4^{2-} greatly exceeds H_2S, the composition of the coexisting C–O–H–S gas phase may be directly calculated from temperature, oxygen fugacity, and water pressure (Whitney, 1984). Using conditions of the Yerington porphyry copper batholith more oxidized than the ilmenite+Ca-pyroxene=magnetite+quartz+titanite buffer (Dilles, 1987; Wones, 1989) yields oxygen fugacities greater than NNO+2.2 log units at 750 °C. The gas in equilibrium with the magma would have a molar SO_2/H_2S of 4:1 at NNO+2.5 log units, and 22:1 at NNO+3 log units; SO_3 gas would be negligible (cf. Carroll and Webster, 1994). Thus, exsolution of an aqueous fluid phase from such a granitic magma yields a fluid dominated by the sulfur species SO_2, which upon cooling undergoes hydrolysis according to the disproportionation reaction

$$4SO_2 + 4H_2O = H_2S + 3H^+ + 3HSO_4^- \quad (2)$$

with hydrogen sulfide, hydrogen, and bisulfate ions the stable end-products of this reaction at 400 to 650 °C. However, these sulfide and bisulfate products of this reaction ultimately serve as the aqueous precursors to the subsequent deposition of sulfide and sulfate minerals. Hereafter, we assume that SO_4^{2-} in the mineral record of the Butte porphyry system was derived from the bisulfate ion product of Eq. (2). Dilles and Field (1996) applied the SO_4^{2-}–H_2S and SO_2–H_2S fractionation equations of Ohmoto and Lasaga (1982) and Ohmoto and Rye (1979) to whole-rock $\delta^{34}S‰$ values of magmatic sulfides to determine the bulk $\delta^{34}S_{\Sigma S}$ value of the Yerington batholith, assuming $SO_2 \gg H_2S$. Analogously, for Butte magmas, we can obtain the bulk-sulfur isotopic composition from

$$\delta^{34}S_{\Sigma S}‰ = 0.25\left(\delta^{34}S_{H_2S}‰\right) + 0.75\left(\delta^{34}S_{SO_4^{2-}}‰\right), \quad (3)$$

by substituting the mean $\delta^{34}S$ values for hydrothermal sulfides and sulfates of the Butte district for those of H_2S and SO_4^{2-} in Eq. (3). The 3:1 molar ratio of SO_4^{2-}/H_2S (HSO_4^-/H_2S of Eq. (2)) is a maximum corresponding to SO_2 as the only sulfur species in the magmatic gas. Under more reduced magmatic conditions, where significant H_2S is evolved from the magma, SO_4^{2-}/H_2S is lower, e.g., a NNO+2.5 oxygen fugacity at 4:1 ratio of SO_2/H_2S in magmatic gas yields a 3:2 ratio of SO_4^{2-}/H_2S in the hydrothermal fluid.

6.2.3. Composition of sulfur in the pre-Main Stage K-silicate assemblage

Anhydrite is an important mineral component of the K-silicate assemblage and is present in most samples collected from DDH-10 of the Pittsmont Dome and Steward mine (4200L) of the Anaconda Dome. Because textural relationships indicate the anhydrite to be largely paragenetically contemporaneous with associated molybdenite, pyrite, and chalcopyrite as veinlets and disseminations, sulfur-isotope analyses of these sulfate–sulfide mineral pairs are useful not simply for purposes of geothermometry, but also in applications to determine $\delta^{34}S_{\Sigma S}$ that require a knowledge of the relative abundances of sulfate and sulfide sulfur. The latter, according to the conventions established by Ohmoto (1972, 1986), Ohmoto and Rye (1979), and Ohmoto and Goldhaber (1997), may be defined by a simplified system

$$X_{SO_4^{2-}} + X_{H_2S} = 1.00 \quad (4)$$

represented by mole fractions of oxidized ($X_{SO_4^{2-}}$) and reduced (X_{H_2S}) sulfur components that sum to unity with respect to total sulfur content. The proportions of these two components are commonly given by the R factor, which is the mole ratio of sulfate to sulfide in the system,

$$R = X_{SO_4^{2-}}/X_{H_2S} \quad (5)$$

but hereafter, this proportion is defined by the sulfate mole fraction ($X_{SO_4^{2-}}$) where

$$X_{SO_4^{2-}} = X_{SO_4^{2-}} \Big/ \left(X_{SO_4^{2-}} + X_{H_2S}\right) = R/(R+1). \quad (6)$$

Field and Gustafson (1976) plotted the $\delta^{34}S$ values of sulfate and sulfide, respectively, versus the $\Delta^{34}S_{sulfate-sulfide}$ value of the mineral pairs in a suite of samples from the porphyry Cu–Mo deposit at El

Salvador, Chile, to demonstrate the potential use of this portrayal for estimates of $\delta^{34}S_{\Sigma S}$ and $X_{SO_4^{2-}}$. Subsequently, this type of plot was applied by Field et al. (1983) to a reconnaissance study of similar hydrothermal deposits elsewhere, and by Kusakabe et al. (1984) to a re-analysis of the El Salvador data and to an extensive isotopic investigation of the Rio Blanco and El Teniente deposits, Chile. Regression analyses of the $\delta^{34}S$ versus $\Delta^{34}S_{sulfate-sulfide}$ ($\delta^{34}S$–$\Delta^{34}S$) data for a suite of sulfate–sulfide mineral pairs of a sample population ideally should form two linear and converging trend lines. Because of the temperature dependency of isotope fractionation, the point of convergence of these two lines extrapolated to infinitely high temperature (>1000 °C and at Δ=0) should define the value for $\delta^{34}S_{\Sigma S}$, and the slopes of the upper and lower lines should approximate the $X_{SO_4^{2-}}$ and X_{H_2S} of the system, respectively (Field and Gustafson, 1976; Kusakabe et al., 1984). The equation for a straight line is

$$y = mx + b \tag{7}$$

where y and x are per mil values of the ordinate ($\delta^{34}S$) and abscissa ($\Delta^{34}S_{sulfate-sulfide}$), respectively, m is the slope, and b is the intercept of the regression lines on the y axis. For the Butte data portrayed in Fig. 3, the positive slope of the $\delta^{34}S_{sulfate}$–$\Delta^{34}S_{sulfate-sulfide}$ line relates to the sulfate mole fraction as

$$X_{SO_4^{2-}} = 1 - m, \tag{8}$$

the negative slope of the $\delta^{34}S_{sulfide}$–$\Delta^{34}S_{sulfate-sulfide}$ line relates to the sulfide mole fraction as

$$X_{H_2S} = 1 + m \tag{9}$$

and the converging lines at intercept (b) on the y axis define $\delta^{34}S_{\Sigma S}$. Assuming an approach to isotopic equilibrium between sulfate and sulfide components, the angle between converging lines of regression is always 45° (provided that the scales of the x and y axes are identical). However, as was illustrated by Field and Gustafson (1976), the position of the upper sulfate $\delta^{34}S$–$\Delta^{34}S_{sulfate-sulfide}$ line changes from nearly +45° (m=1) to nearly horizontal as $X_{SO_4^{2-}}$ ranges from nil (≤0.05) to near unity (≥0.95), whereas the complementary lower sulfide $\delta^{34}S$–$\Delta^{34}S_{sulfate-sulfide}$ line changes from nearly horizontal to nearly −45° (m=−1) as X_{H_2S} ranges from near

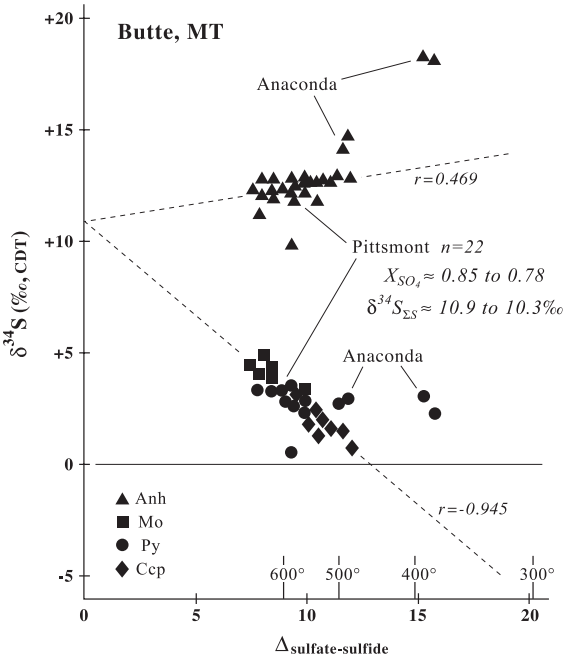

Fig. 3. Plot of $\delta^{34}S$‰ values for associated sulfate (anhydrite) and sulfides of mineral pairs versus the delta (Δ) value of the pair from veinlets in samples of the pre-Main Stage K-silicate assemblage of the Anaconda and Pittsmont domes. Provided several constraints have prevailed, the convergence and slopes of the two regression lines may offer an approximation of the bulk sulfur isotopic composition ($\delta^{34}S_{\Sigma S}$) and the proportion of oxidized to reduced sulfur ($X_{SO_4^{2-}}$ to X_{H_2S}) in the hydrothermal system.

unity (≥0.95) to nil (≤0.05). Thus, as noted by Ohmoto (1972, and thereafter), as the oxidized or reduced form of sulfur becomes the dominant component (X_i≥0.90), its isotopic composition approaches that of $\delta^{34}S_{\Sigma S}$ in the system.

The reliability of this portrayal requires having a representative suite of coexisting (contemporaneous) sulfate–sulfide mineral pairs that were deposited over a range of temperatures; that isotopic equilibrium prevailed at the time of deposition and was retained thereafter; that the $X_{SO_4^{2-}}$ remained relatively constant; and that the $\delta^{34}S_{\Sigma S}$‰ composition of the system remained unchanged because of an infinite sulfur reservoir, lack of contamination from an isotopically distinct extraneous source, or abrupt perturbations caused by various magmatic processes or related catastrophic events (Field and Gustafson, 1976; Field et al., 1983; and further critical discussions by Ohmoto, 1986; Seal et al., 2000). The particular

concerns of those authors are the vagaries of natural systems, especially with respect to isotopic equilibrium, and the mathematical basis of the converging regression lines that implies an induced correlation. Nonetheless, this treatment may be valid in studies of sulfate–sulfide assemblages from porphyry-type deposits because isotopic equilibrium is favored by the high temperatures of this environment as inferred from the close relationships to igneous rocks, associated K-silicate alteration, characteristics of the fluid inclusions, and from the measured fractionations and calculated isotopic temperatures.

6.2.4. Bulk-sulfur isotopic composition derived from the Pittsmont Dome

Distributions of the $\delta^{34}S$ and $\Delta^{34}S$ values for 27 sulfate–sulfide mineral pairs are plotted on Fig. 3 for samples of the K-silicate assemblage from the Pittsmont and Anaconda domes. The plot of the four samples from the Anaconda Dome seems to represent a population distinct from that of the Pittsmont Dome. With the exception of one sulfate–sulfide mineral pair from the Pittsmont Dome (sample 11172-2460.5; Table 1), the other 22 pairs exhibit a fair linear distribution, and the calculated sulfate and sulfide $\delta^{34}S$–$\Delta^{34}S$ regression lines converge at the ordinate (Δ=0) to a value of 10.9‰ for $\delta^{34}S_{\Sigma S}$. This value is remarkably similar to the 9.9‰ calculated from Eq. (3) using values for $X\mathrm{SO}_4^{2-}$ and $X\mathrm{H}_2\mathrm{S}$ of 0.75 and 0.25, respectively, and derived from the disproportionation reaction for SO_2 hydrolysis (Eq. (2)) and the mean $\delta^{34}S$ values for anhydrite and sulfides from the Pittsmont Dome. In addition, the slopes of the two regression lines on Fig. 3 provide calculated values for $X_{SO_4^{2-}}$ and X_{H_2S} of 0.85 and 0.15, respectively. These lines of regression and mole fractions have been calculated using the per mil values of the sulfide minerals. However, if they are recalculated using the isotopic compositions of H_2S that equilibrated with these sulfides, based on the isotopic temperature estimates (Table 3), the recalculated $\delta^{34}S_{\Sigma S}$ is 10.3‰ and SO_4^{2-} and H_2S mole fractions are 0.78 and 0.22, respectively. The latter mole-fraction estimates are in close agreement with those dictated by Eq. (2), and used in the calculation of $\delta^{34}S_{\Sigma S}$ with Eq. (3), which yields a maximum $X_{SO_4^{2-}}$. The mole fractions also are consistent with those determined from modal analyses of anhydrite and sulfides in K-silicate alteration by Roberts (1975; up to 5 vol.% anhydrite and average 2 vol.% sulfide) and in 'early dark mica' veinlet selvages by Brimhall (1977; SO_4^{2-}/H_2S mole ratio of 2 to 3). Sample 11172-2460.5 is isotopically anomalous (anhydrite=9.8 and pyrite=0.5‰), but potentially significant. The data were omitted from calculations of the regression lines for the Pittsmont Dome samples because both the anhydrite and pyrite are anomalously depleted in $\delta^{34}S$ relative to their counterparts elsewhere in this dome (Fig. 3), and because the paragenetic relationship could not be established with certainty. The quartz/anhydrite ratio of the veinlet approximates 20 to 30, whereas the sulfide is present only in trace amounts, with anhydrite/pyrite≥100. Should this mineral ratio approximate the SO_4^{2-} mole fraction of the hydrothermal fluid ($X_{SO_4^{2-}} \approx 0.99$) from which these minerals were deposited, then the per mil value of $\delta^{34}S_{\Sigma S}$ must be similar to that of the anhydrite (9.8‰). It is difficult to assess this apparent agreement for these independent approximations of $\delta^{34}S_{\Sigma S}$ and $X_{SO_4^{2-}}$. The linearity of regression lines in Fig. 3 is largely a consequence of differences related to increasingly larger delta values (decreasing temperatures), as previously noted, in the succession of mineral pairs from anhydrite–molybdenite, through anhydrite–pyrite, to anhydrite–chalcopyrite. Moreover, these differences remain, although they become smaller, when the sulfide–mineral per mil values are recalculated to those of their coexisting H_2S precursor.

Another useful variant to the illustration of these sulfur-isotope data is provided by a $\delta^{34}S$-sulfate versus $\delta^{34}S$-sulfide ($\delta^{34}S_{SO_4^{2-}}$–$\delta^{34}S_{H_2S}$) diagram. Again, this representation offers a visual portrayal of $X_{SO_4^{2-}}$ and $\delta^{34}S_{\Sigma S}$ as determined from the usual statistical parameters of regression analysis, and it serves additionally as a means for comparing the data of geographically or temporally distinct mineral deposits. The rationale for this diagram is given in Fig. 4A, which illustrates the possible evolutionary trajectories of $\delta^{34}S$ in sulfate–sulfide pairs of a hydrothermal system with decreasing temperature, changes in $X_{SO_4^{2-}}$, and at constant $\delta^{34}S_{\Sigma S}$ values of either 0 or 10‰, respectively. A system having $\delta^{34}S_{\Sigma S}$ of 0‰ under relatively reducing conditions ($X_{SO_4^{2-}} \approx 0.05$) and over the temperature range of 600 to 300 °C will deposit sulfides that vary from about −0.5‰ to −1.0‰, and will deposit coexisting sulfates that vary from about

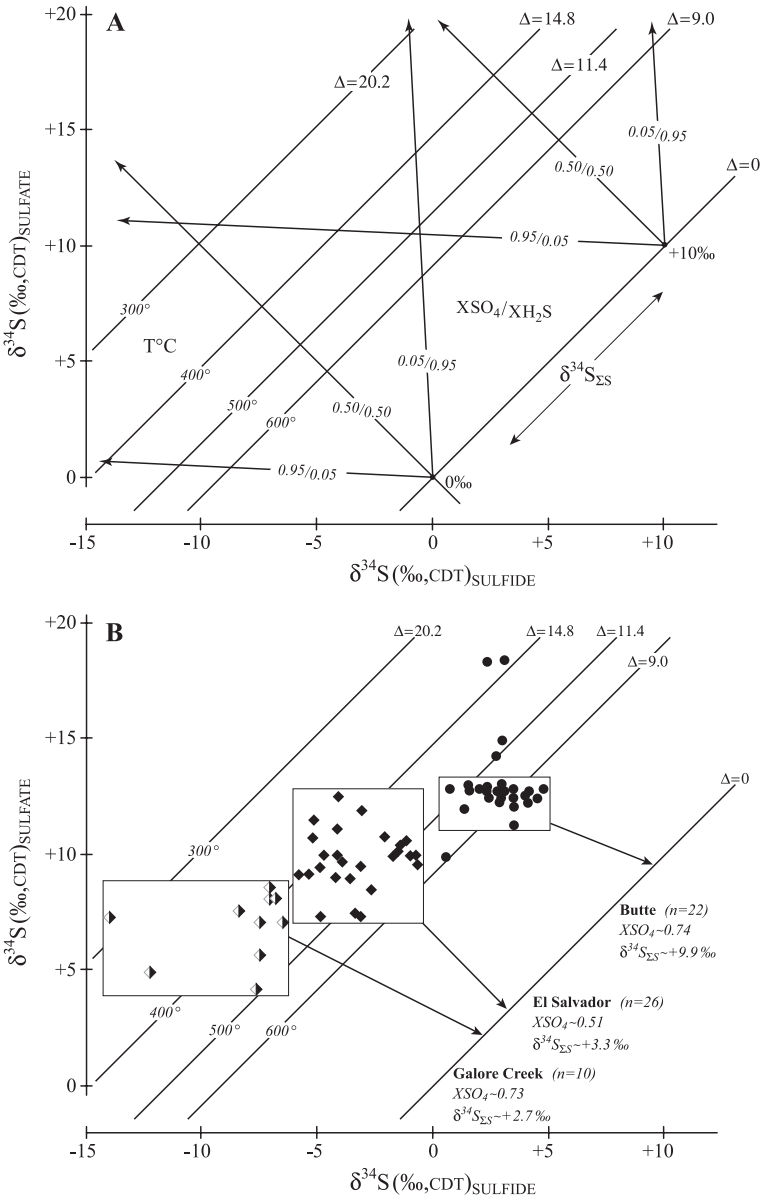

Fig. 4. (A) Plot of $\delta^{34}S_{SO_4^{2-}}$ versus $\delta^{34}S_{H_2S}$ that shows the potential range of isotopic variations caused by changes in temperature (300 to 600 °C and higher), changes in the proportion of oxidized to reduced sulfur ($X_{SO_4^{2-}} \approx 0.05, 0.50,$ and 0.95), and changes in the isotopic composition of bulk sulfur ($\delta^{34}S_{\Sigma S} \approx 0‰$ or 10‰) in the hydrothermal system. (B) Plot of $\delta^{34}S$ for anhydrite or gypsum versus $\delta^{34}S$ for molybdenite, pyrite, or chalcopyrite of the porphyry deposits at Butte, Montana, Galore Creek, British Columbia, and El Salvador, Chile. The isotopic domains and regression statistics of the data suggest that the deposits are sulfate-rich ($X_{SO_4^{2-}} \geq 0.50$) and have bulk sulfur ($\delta^{34}S_{\Sigma S}$) compositions that may range from ≈3‰ to ≈10‰.

8.6‰ to 19.2‰. In contrast, a more oxidized equivalent of this system ($X_{SO_4^{2-}} \approx 0.95$) over this same temperature range will deposit sulfides that vary from about −8.6‰ to −19.2‰, and sulfates that vary from about 0.5‰ to 1.0‰. With subequal amounts of reduced and oxidized sulfur in this system, the compositions will vary from about −4.5‰ to −10.1‰ for sulfides, and from about 4.5‰ to

10.1‰ for sulfates. However, if the value of $\delta^{34}S_{\Sigma S}$ is taken to be 10‰ (Fig. 4A), and conditions of temperature and $X_{SO_4^{2-}}$ as previously enumerated are retained, then the fractionations between sulfates and sulfides remain the same, but the isotopic values of these minerals increase by 10‰. Isotherms for SO_4^{2-}–H_2S equilibria show that isotopic fractionation between sulfate and sulfide remains the same at constant temperature, regardless of changes in $\delta^{34}S_{\Sigma S}$. Nonetheless, at constant temperature and constant $\delta^{34}S_{\Sigma S}$, the absolute per mil values of these minerals will change with variations in $X_{SO_4^{2-}}$. Isotopic trajectories at constant $X_{SO_4^{2-}}$ projected up thermal gradients to the infinitely high temperature isotherm (where $\Delta \approx 0$) converge on the value for $\delta^{34}S_{\Sigma S}$.

An important feature of isotope systematics, as described in the previous paragraph and first enunciated by Ohmoto (1972), is portrayed in Fig. 4A. As the oxidized or reduced species of sulfur becomes the more abundant component of a system, the $\delta^{34}S$ values of this component become less variable over a given temperature range and approach that of $\delta^{34}S_{\Sigma S}$. In contrast, the $\delta^{34}S$ values of the minor component become more variable in response to temperature-induced fractionation. This differential isotopic effect, which relates to proportions of oxidized to reduced sulfur, provides a rapid means of approximating the $X_{SO_4^{2-}}$ for a deposit. The effect is determined simply by comparing the spread of $\delta^{34}S$ values within sulfate and sulfide fractions of the sample suite as follows,

$$X_{SO_4^{2-}} = \Delta\delta^{34}S_{H_2S} \Big/ \left(\Delta\delta^{34}S_{SO_4^{2-}} + \Delta\delta^{34}S_{H_2S}\right) \quad (10)$$

wherein Δ is the isotopic spread (difference or separation) between the highest and lowest $\delta^{34}S$‰ values from the analytical data for each fraction, or preferably from standard deviations calculated therefrom. Application of Eq. (10) to the Butte data for 22 sulfate–sulfide pairs from the Pittsmont Dome gives $X_{SO_4^{2-}}$ values of 0.71 and 0.73 using differences in the raw $\delta^{34}S$‰ data and standard deviations, respectively. Alternatively, a single value of 0.67 is obtained from either procedure if the sulfide data are recalculated to those of their H_2S precursors. With regression analysis of the sulfate–sulfide mineral pair data, $X_{SO_4^{2-}}$ is calculated to be 0.95 from Eq. (6), because R is equal to $1/m$ on the $\delta^{34}S_{SO_4^{2-}}$–$\delta^{34}S_{H_2S}$ diagram (also see Eqs. (5) and (7)). Additionally, regression analysis provides two interrelated means by which to estimate $\delta^{34}S_{\Sigma S}$. The fastest is to extrapolate graphically the $\delta^{34}S_{SO_4^{2-}}$–$\delta^{34}S_{H_2S}$ regression line from the b (y axis) intercept using the calculated m (slope) value, or from the b intercept through the mean $\delta^{34}S$‰ values for sulfates and sulfides comprising the mineral pairs, to its intersection with the high-temperature (Δ=0) isotherm. Alternatively, statistical data from the regression analysis may be used in the equation

$$\begin{aligned}\delta^{34}S_{\Sigma S} &= \delta^{34}S_{SO_4^{2-}} - \left(\Delta_{SO_4^{2-}-H_2S}\right)\left(1 - X_{SO_4^{2-}}\right) \\ &= \delta^{34}S_{H_2S} - \left(\Delta_{SO_4^{2-}-H_2S}\right)\left(X_{H_2S} - 1\right)\end{aligned} \quad (11)$$

where $\delta^{34}S_{SO_4^{2-}}$ and $\delta^{34}S_{H_2S}$ are the mean per mil values for sulfate- and sulfide-mineral fractions, respectively, and their difference is $\Delta^{34}S_{SO_4^{2-}-H_2S}$. An unlikely large value for $\delta^{34}S_{\Sigma S}$ of 11.9‰ is obtained using either graphic or computational method because of the unreasonably large value for $X_{SO_4^{2-}}$ (0.95) derived from regression analysis as described above. Significant differences are commonly obtained in the calculated values for $X_{SO_4^{2-}}$ ($\pm$0.10) and $\delta^{34}S_{\Sigma S}$ ($\pm$1.0) that are dependent on the method of estimation and linearity of the data. In particular, the $\delta^{34}S_{SO_4^{2-}}$–$\delta^{34}S_{H_2S}$ regression data provide the largest estimated values for $X_{SO_4^{2-}}$ and $\delta^{34}S$-enriched $\delta^{34}S_{\Sigma S}$. These estimates must be viewed with caution because of the covariance of $X_{SO_4^{2-}}$ with $\delta^{34}S_{\Sigma S}$ (Fig. 4A), and as dictated by the requirement of isotopic balance in Eqs. (3) and (11). The most conservative estimates of these parameters are readily calculated from the means, ranges, and (or) standard deviations of the sulfate and sulfide data, which are then entered in Eqs. (10) and (11).

The sulfate–sulfide data for deep pre-Main Stage porphyry-type mineralization of the Anaconda and Pittsmont domes are illustrated in Fig. 4B, as are the equivalent data for similar deposits of Galore Creek, British Columbia (Field et al., 1983) and El Salvador, Chile (Field and Gustafson, 1976) for which additional data are included. Rectangular areas enclose the sulfate–sulfide $\delta^{34}S$ data of mineral pairs and define the isotopic domains for the Pittsmont Dome and the other two deposits. Also listed are "best" estimates of $X_{SO_4^{2-}}$ and $\delta^{34}S_{\Sigma S}$ based on the methods and uncertainties previously cited. The plotted distributions of the samples in $\delta^{34}S_{SO_4^{2-}}$–$\delta^{34}S_{H_2S}$ space vary

from district to district. Those of the Pittsmont Dome exhibit the most linear distribution and narrowest range of $\delta^{34}S$ values and temperatures. This isotopic feature is consistent with the more restricted geological environment from which sulfate–sulfide pairs of the Pittsmont Dome were collected, i.e., a continuous vertical interval in a single diamond-drill hole, and to one host rock that has been subjected to a largely uncomplicated, K-silicate episode of hydrothermal alteration and metallization (porphyry Cu–Mo). In contrast, the sample suites from El Salvador and Galore Creek are more diverse with respect to district-wide geography, geology, and imposed hydrothermal environments. Thus, the isotopic data for these deposits are more variable and occupy larger domains. The crude linearity and nearly flat negative slope displayed by most of the sample data for the Pittsmont suite suggest a dominantly temperature-induced isotopic trend at relatively large values for $X_{SO_4^{2-}}$ ($\approx$0.74, or more) and $\delta^{34}S_{\Sigma S}$ (9.9‰ or more). However, the data for Galore Creek, and especially El Salvador, are more broadly dispersed with respect to both sulfate and sulfide, which suggests that variations in $X_{SO_4^{2-}}$ and possibly $\delta^{34}S_{\Sigma S}$, in addition to temperature, are collectively responsible for the scatter. Note also that the square to horizontally rectangular shapes of the $\delta^{34}S$ domains for each of the three deposits are entirely compatible with the large $X_{SO_4^{2-}}$ values ($\geq$0.50) estimated from calculations and inference (Fig. 4A,B). The isotopic data for mineral pairs formed in systems having $X_{SO_4^{2-}}$ values of less than 0.50 would be increasingly defined by vertically aligned rectangular domains.

With the exception of Yerington, Nevada (Dilles and Field, 1996), the surprisingly ^{34}S-enriched and estimated value of about 9.9‰ for $\delta^{34}S_{\Sigma S}$ of the Pittsmont Dome is heavier than the generally accepted range of ~0±3‰ to 5‰ for magmatic sulfur, and especially from silicic to intermediate igneous rocks of the western U.S. (Ohmoto and Rye, 1979; Ohmoto and Goldhaber, 1997). Distributions of the data into distinct and separate isotopic domains in Fig. 4B suggest that each of the three hydrothermal systems is defined by a generally distinct value of $\delta^{34}S_{\Sigma S}$. It is theoretically possible to derive all data points in Fig. 4B from a system having a $\delta^{34}S_{\Sigma S}$ composition of about 5‰ by simply varying $X_{SO_4^{2-}}$ from about 0.99 to 0.01 to produce the isotopic array extending from Galore Creek, through El Salvador, to Butte (Pittsmont Dome). Such a model conflicts with geological reality because it requires Butte to become a SO_4^{2-} deficient system, which it is not, and the implied reduced state would also render the subhorizontal isotopic linearity unlikely (compare Fig. 4A and B).

In summary, it is difficult to assess the true merits of the two data portrayals as illustrated in Figs. 3 and 4, without more examples. The $\delta^{34}S$ versus $\Delta^{34}S_{sulfate-sulfide}$ plot commonly provides better regression statistics, which may be attributed to mathematical problems caused by the restricted range of the $\delta^{34}S$ values for these porphyry-type deposits (see Seal et al., 2000), and values for $X_{SO_4^{2-}}$ and $\delta^{34}S_{\Sigma S}$ are more consistently reasonable. However, the plot of $\delta^{34}S_{sulfate}$ versus $\delta^{34}S_{sulfide}$ (Fig. 4A) shows the isotopic effects of temperature and $X_{SO_4^{2-}}$ clearly, and is ideal for discriminating between local and regional isotopic domains, including those of the Anaconda and Pittsmont domes of this study (Fig. 4B).

6.2.5. Source of ^{34}S enrichment in the K-silicate system and Butte magmas

A relevant topic concerns the source or cause of the apparent ^{34}S enrichment (about 9.9‰) of $\delta^{34}S_{\Sigma S}$ in minerals of the Pittsmont Dome. As shown by field relations (Reed, 1980, 1999), petrological studies (Roberts, 1975; Brimhall, 1977), and the anhydrite–sulfide isotopic data herein, this mineralization took place at a high temperature of ~550–600 °C and in close temporal and spatial association with quartz porphyry dikes. Hence, the responsible hydrothermal fluids were of magmatic origin, and in places 'early dark mica'-related biotite–chalcopyrite breccias can be directly traced to sources in porphyry dikes (Reed, 1999). Thus, sulfur is directly derived from these porphyries of granitic composition.

Sulfur originally present in a deep-seated magmatic system derived from a mantle-sourced basalt would have had an initial isotopic composition of approximately 0±3‰ (cf. Ohmoto and Rye, 1979). The observed ^{34}S enrichment at Butte might be accomplished by degassing processes that are normally associated with hydrous magmas. For oxidized magma (oxygen fugacity ~NNO+2.5 log units) such as the Butte quartz porphyries, application of the Rayleigh fractionation sulfur-degassing models of Mandeville et al. (1996) together with S–O–H gas

speciation ($X_{SO_4^{2-}}$=0.8, X_{H_2S}=0.2) at 750 °C and 200 MPa yields $\Delta^{34}S_{magma-gas}$=~3.5‰. Therefore, production of a daughter melt with a $\delta^{34}S$ of 10‰ ^{34}S from a parent 0‰ source would require a 93% loss of the original sulfur by way of open-system degassing. We conclude that this amount of degassing is extremely unlikely, based on two principal arguments: (1) the earliest record of magmatic degassing at Butte is recorded in the pre-Main Stage 'early-dark micaceous' and related veins, which have $\delta^{34}S_{\Sigma S}$ values ≈ 10‰ and $\delta^{34}S$<0‰; and (2) mass-balance calculations suggest that sulfur deposited in the pre-Main Stage 'early dark micaceous' assemblages and related assemblages represent complete degassing of a magma batch, rather than the last 5% to 20%. For example, the pre-Main Stage contains ~30 M tonnes of Cu metal (Long, 1995), and this yields an estimate of 300 to 600 M tonnes of S deposited using a mineralogical estimate of the Cu/S weight ratio between 1:10 and 1:20.

We prefer the interpretation that quartz porphyry magmas related to pre-Main Stage ores were ^{34}S-enriched because of crustal contamination during the formation of these granitic magmas. The most likely mechanism of ^{34}S enrichment is through magmatic assimilation of isotopically heavy marine evaporite sulfate. The contamination hypothesis is potentially viable because Claypool et al. (1980) have demonstrated that most Proterozoic and Phanerozoic marine evaporites are enriched in ^{34}S (range of 10‰ to 35‰), widespread, and thus constitute a realistic crustal source of heavy sulfur. In addition, compilations by Stearn et al. (1979), Blatt et al. (1980), and Ehlers and Blatt (1982) record the presence of anhydrite-bearing evaporites of Mississippian age in southwestern Montana. Sulfates of this age may range from about 14‰ to 20‰ (Claypool et al., 1980).

The most realistic source of magmatic contamination is evaporites within the middle Proterozoic Belt Supergroup, through which the Boulder batholith has been emplaced (Harrison, 1972). There is direct evidence that Belt-type rocks are contaminants because most of the zircon samples analyzed for U and Pb within the quartz porphyry dikes at Butte are Proterozoic in age (~1.5 to 2.5 Ga) with narrow late-Cretaceous rims (Martin et al., 1999; Lund et al., 2002; J.H. Dilles, unpublished data). The Missoula Group in the upper part of the Belt includes redbed siltstones and mudstones, locally with salt casts, that are indicative of shallow marine to supratidal conditions (cf. Smith and Barnes, 1966). Evaporite sulfate has not been observed within the Belt Supergroup, but the presence of salt casts suggests that supratidal deposits originally contained gypsum. Barite that is inferred to replace primary evaporitic gypsum and anhydrite has $\delta^{34}S$ of 13.6‰, 14.4‰, and 18.3‰ in the Newland Formation near Butte (Strauss and Scheiber, 1990) and 28.6‰ and 32.3‰ in the Altyn Formation (Chandler and Gregoire, 2000). Lyons et al. (2000) have reported that the diagenetic pyrite in the Newland Formation has $\delta^{34}S$ ranging from −8.7‰ to 36.7‰ (mean=7.6‰, n=41), and interpreted these sulfides as produced by bacterial reduction of seawater sulfate. In addition, isotopically heavy sulfur occurs in sulfides in the Spar Lake and related Cu–Ag and Co deposits hosted in the Belt Supergroup west of Butte. The Spar Lake deposit formed shortly after early diagenesis of host siltstones of the Revett Formation when oxidized, low-salinity, sulfate- and Cu–Ag–Co-bearing fluids encountered reduced rocks that precipitated Cu and Cu–Fe sulfides at 50–150 °C with $\delta^{34}S$ values ranging from 3‰ to 23‰ (Hayes and Einaudi, 1986; Hayes et al., 1989).

The regional relationships of Butte and the Boulder batholith to rocks of the Belt Supergroup and its salt casts and stratabound sulfide deposits are compiled in Fig. 5. Thus, the Belt Supergroup contained ^{34}S-enriched evaporite sulfate, diagenetic pyrite, and hydrothermal sulfide that represent the potential crustal contaminants to Butte quartz porphyry magmas. The Belt source would be sufficient to raise $\delta^{34}S_{\Sigma S}$ from a mantle-like value of 0‰, to 10‰ when assimilated crustal sulfur combined and equilibrated with a subequal or lesser amount of magmatic sulfur in the Pittsmont system; use of 0‰ and 14‰ as the mixing end-members yields an ~71% crustal source of sulfur for the Butte magma.

6.2.6. Brine–vapor unmixing model for sulfur fractionation in the Anaconda Dome

The sulfur isotopic data for anhydrite from the Pittsmont Dome are relatively uniform (12.3±0.4‰, n=18), whereas the data for four samples from the Anaconda Dome are isotopically heavier and range widely from 14.1‰ to 18.2‰. The four anhydrite–pyrite pairs from the Anaconda Dome (Figs. 3 and 4)

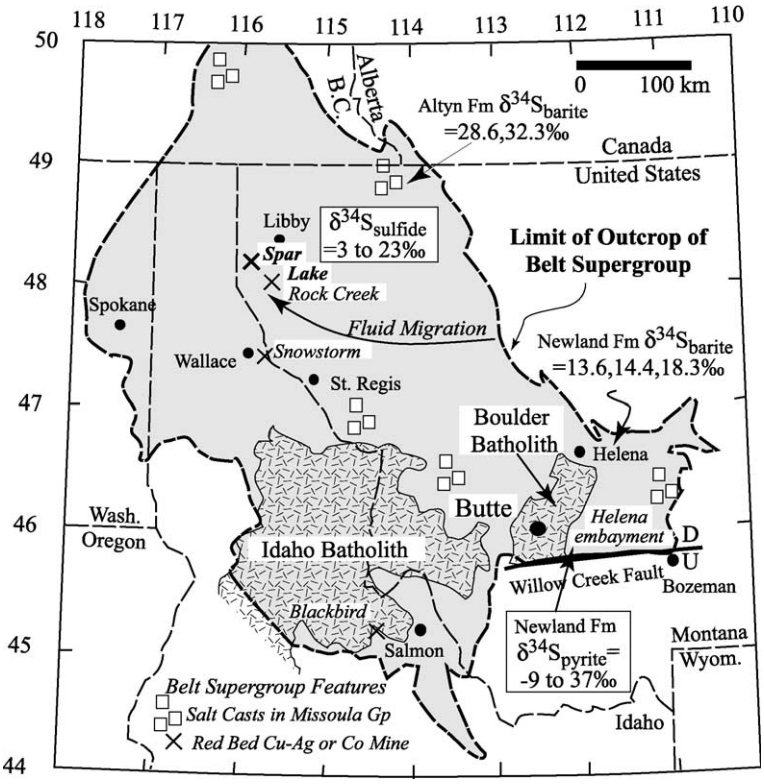

Fig. 5. Location of the Butte district, showing emplacement of the Boulder batholith into clastic sedimentary rocks of the middle and upper Proterozoic Belt Supergroup (after Harrison, 1972). The Missoula Group contains salt clasts indicative of evaporite conditions (Smith and Barnes, 1966). Post-diagenetic Cu and Cu–Fe sulfides at Spar Lake and other Cu–Ag and Co deposits have ^{34}S-enriched isotopic compositions; fluid flow was to the northwest (Hayes et al., 1989).

seem to represent an isotopically different population because the anhydrite fractions, but not the pyrite, are variably enriched in ^{34}S relative to their counterparts from the Pittsmont Dome. Delta values for these pairs are moderately larger and, accordingly, yield lower isotopic temperatures of 360 to 475 °C (Table 3). Anhydrite in samples Bu-8a and -8b has the isotopically heaviest sulfur (18.2‰ and 18.1‰, respectively), gives the largest delta values (15.2‰ and 15.8‰, respectively), and provides the lowest temperatures (370 and 360 °C, respectively) of any Butte anhydrite–sulfide pairs. Sample suites of the Pittsmont and Anaconda domes also differ because those of the former come largely from veinlets of the 'early dark micaceous' type wherein fluid inclusions are of simple liquid plus vapor, whereas samples from the Anaconda Dome come from 'early dark micaceous' and 'pale green sericitic' veinlets that contain both halite-bearing inclusions with a small vapor bubble and vapor-rich fluid inclusions (Rusk, 2003; Rusk et al., 2004). The Pittsmont samples represent an approximately 1 km greater depth of trapping. Rusk et al. (2004) interpreted these inclusions to contain a single-phase magmatic fluid, with 4 to 5 wt.% NaCl, that was trapped in the deeper parts of the Pittsmont Dome. Similar fluid in the shallower Anaconda Dome ascended, depressurized so as to intersect the water–NaCl solvus, and unmixed into separate brine and low-salinity vapor phases (cf. Bodnar et al., 1985; Hedenquist and Lowenstern, 1994), which were trapped as the halite-bearing and vapor-rich inclusions, respectively.

The brine–vapor unmixing may have led to sulfur isotopic fractionation, as outlined below. As noted earlier, SO_2 is the principal sulfur species in gases evolved from most oxidized porphyry-Cu

magmas. As illustrated by Eq. (2), SO_2 in the parental magmatic–hydrothermal fluid disproportionates via reaction with water at temperatures beginning at about <700 °C, and goes to completion by ~400 °C, to yield H_2SO_4 and H_2S in the molar proportion of 3:1 (XSO_4^2=0.75). We estimate that, at Butte, disproportionation of SO_2 took place at higher temperature than the 400 °C typically taken as the upper limit (Ohmoto and Rye, 1979) based on two arguments. First, the fluids that formed Butte's deep 'early dark micaceous' assemblage were trapped at high pressure, and calculations using SUPCRT92 (Johnson et al., 1992) at pH estimated from Hemley et al. (1992) indicate that disproportionation equilibrium increases by ~100 °C as pressure increases from 500 to 2000 bar. Second, K-silicate reactions at 500 to 600 °C, such as conversion of hornblende to biotite and anhydrite, and conversion of feldspar to muscovite, andalusite, and corundum (Brimhall, 1977; Brimhall et al., 1985) require consumption acid and bisulfate and therefore cause reactions (2) and (3) to proceed to the right, causing additional SO_2 disproportionation. This theoretical ratio is in agreement with isotopic estimates of $X_{SO_4^{2-}}$=~0.71-0.77 for the Pittsmont samples and with molar sulfate/sulfide between 3:1 and 2:1 ($X_{SO_4^{2-}}$ of 0.75 to 0.67) for sulfur precipitated as anhydrite and sulfide as determined for 'early dark micaceous' veinlets and selvages (Brimhall, 1977). When a single-phase magmatic–hydrothermal fluid unmixes into brine and vapor, H_2S is proportioned both into the brine as an aqueous species and into the low-density vapor as a gaseous species. In contrast, SO_4^{2-} remains entirely in the brine phase because it does not form a gaseous species. The partition coefficient for H_2S between brine and vapor is unknown, but a reasonable value might be ~1 on the basis of the close association of Cu with H_2S and the observed partition coefficient of ~1 for Cu between brine and vapor at the Bajo Alumbrera porphyry-Cu deposit (Ulrich et al., 2001). Because H_2S is depleted in ^{34}S relative to SO_4^{2-}, removal of the H_2S-bearing vapor would leave the remaining sulfate-rich brine enriched in ^{34}S. Although small amounts of SO_2 gas would be present in the vapor at 400 to 550 °C, the gas would be subordinate to other sulfur species. Loss of SO_2 gas to the vapor would have an isotopic effect similar to that of H_2S, but the amount of ^{34}S enrichment imposed on the sulfate-rich brine per unit loss would be markedly less.

As illustrated in Fig. 6, loss of 13% to 52% of the sulfur as a H_2S-rich vapor would produce the observed range of ^{34}S-enriched anhydrite compositions (14.1‰ to 18.2‰) at 550 °C and ~600 to 700 bar (6 to 7 km depth under hydrostatic conditions) if the R ratio (SO_4^{2-}/H_2S) of the brine is fixed at 3:1 ($X_{SO_4^{2-}}$=0.75). This ratio reflects that likely to have been present initially in the brine, but removal of H_2S to vapor would be expected to decrease the ratio. However, we here assume that the Fe in fluid and wallrock buffers the oxygen fugacity of the brine and, therefore, the SO_4^{2-}/H_2S ratio. These Fe-buffers would allow SO_4^{2-} in the brine to be reduced to H_2S via a coupled oxidation of ferrous to ferric iron. Several Fe-bearing minerals that crystallized in the 'pale green sericitic' and 'early dark micaceous' assemblages could accomplish the proposed reduction of sulfate. Notably, the zones of 'pale green sericitic' alteration contain the highest Cu grades and chalcopyrite contents of the pre-Main Stage zones, 2–4 wt.% pyrite, and the bulk of magnetite (up to 5 wt.%) as indicated by the magnetite vein zone (Fig. 1B). The following coupled reactions would reduce sulfate to sulfide and precipitate magnetite, pyrite, and chalcopyrite:

$$12FeCl_2 + 12H_2O + H_2SO_4 = 4Fe_3O_4 + 24HCl + H_2S \quad (12)$$

$$4FeCl_2 + 7H_2S + H_2SO_4 = 4FeS_2 + 8HCl + 4H_2O \quad (13)$$

$$8CuCl + 8FeCl_2 + 15H_2S + H2SO_4 = 8CuFeS_2 + 24HCl + 4H_2O \quad (14)$$

Note that reactions (12)–(14) also release acid as HCl on the right-hand side of the equations. Generation of acid is consistent with abundant sericitic replacement of feldspar in 'pale green sericitic' selvages, in contrast to the higher temperature 'early dark mica' selvages, wherein 'sericite' is sparse (Brimhall, 1977; Roberts, 1973; Reed, 1980).

The numerical model for Butte sulfate data suggests that brine–vapor immiscibility allows ^{34}S-depleted H_2S to be removed in the buoyant low-density vapor so that the remaining brine becomes ^{34}S-enriched via Rayleigh-type fractionation (Fig. 6). The data for Pittsmont sulfate suggest that 'deep'

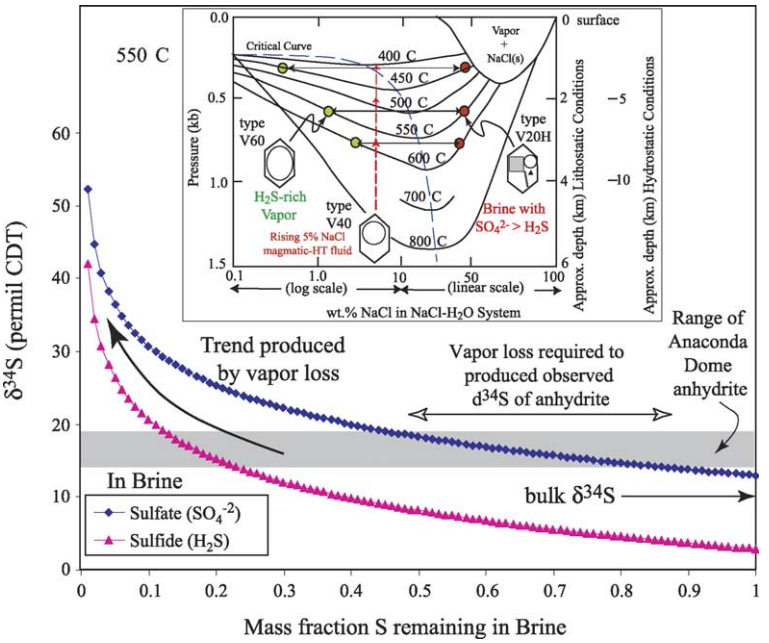

Fig. 6. Model for loss of H_2S-rich and ^{34}S-depleted vapor from brine that illustrates the $\delta^{34}S$ composition of residual H_2S and SO_4^{2-} remaining in brine from the Anaconda Dome. Temperatures are approximate and are estimated from stable-isotope, fluid-inclusion, and petrologic data. The Rayleigh fractionation model at 550 °C (with $\Delta_{SO_4^{2-}-H_2S} = 10.1‰$) assumes that oxygen fugacity is buffered by wallrock so that SO_4^{2-} remaining in the brine is continually reduced to H_2S to keep the ratio of H_2S/SO_4^{2-} fixed at 1:3 (see text). Inset shows the water–NaCl phase equilibria as a function of pressure and composition contoured for temperature of the two-phase immiscibility surface (after Bodnar et al., 1985). Butte magmatic–hydrothermal fluids would begin to unmix at depths of 6 to 7 km at 600 °C at hydrostatic pressures. Separation of 13% to 52% of the sulfur as a low-density H_2S-rich vapor from the brine could fractionate sulfur isotopes as modeled so that the remaining sulfate might produce the observed range of anhydrite $\delta^{34}S$ values (14.1‰ to 18.2‰).

anhydrite has rather uniform $\delta^{34}S$ compositions, consistent with a high ratio of sulfate to sulfide and with the presence of a single hydrothermal fluid phase at 550 to 600 °C. As an ascending fluid drops to hydrostatic pressures (Rusk and Reed, 2002), it unmixes to vapor and brine, and the sulfur isotopic fractionation leads to progressive ^{34}S enrichment of the brine and the precipitated anhydrite, as observed in the Anaconda Dome. The sample calculation for 550 °C illustrates this process at 600–700 bar (Fig. 6), but similar fractionation can occur at lower temperature (450 °C) and at 300–400 bar. The isotopic temperatures for anhydrite–pyrite from the Anaconda Dome suggest deposition at 360 to 475 °C from the brine phase. However, the total H_2S removed in the vapor (average 2‰ to 4‰) would be isotopically lighter than that remaining in the brine, and if the vapor contributed sulfur to the precipitated sulfides, isotopic disequilibrium would prevail and the resulting temperatures from anhydrite–pyrite would be too low. Comparisons with other porphyry-Cu deposits that have brine and vapor-rich fluid inclusions suggest that large ranges of anhydrite $\delta^{34}S$ compositions are common (cf. Galore Creek and El Salvador, Fig. 4). Thus, brine–vapor unmixing and consequent sulfur isotopic fractionation possibly is a common process in porphyry hydrothermal systems.

The four samples from ‘early dark micaceous’ and ‘pale green sericitic’ veinlets of the Anaconda Dome that illustrate the wide range of isotopic compositions in anhydrite have a restricted range of compositions for pyrite: $\delta^{34}S = 2.7 \pm 0.3‰$, 1 S.D., $n=4$. These data are consistent with the processes outlined above, and specifically suggest that in these samples $X_{SO_4^{2-}} = \leq 0.5$, reflecting Fe reduction of sulfate, and that the temperature was a relatively low ~400 to 500 °C. Modeling at 450 °C suggests that, after one-third of the sulfur has been extracted by the vapor as H_2S with an average $\delta^{34}S_{H_2S} \approx 1.4‰$, the remaining sulfate has $\delta^{34}S_{SO_4^{2-}} \approx 16.5‰$ and $X_{SO_4^{2-}} \approx 0.5$. Thus, with the

lowering of temperature in pre-Main Stage alteration as depicted in Fig. 7, $X_{SO_4^{2-}}$ decreases but the $\delta^{34}S_{H_2S}$ of pyrite and other sulfides stays relatively constant because the $\delta^{34}S_{SO_4^{2-}}$ of aqueous sulfate and anhydrite increases sharply.

6.2.7. Composition of sulfur in fluids of the pre-Main Stage 'gray-sericitic' and Main Stage assemblages

The sulfur isotopic compositions of pyrite and other sulfides in the pre-Main Stage 'gray-sericitic' assemblage and younger Main Stage mineralization are similar to those of the earlier pre-Main Stage K-silicate assemblage; calculated mean $\delta^{34}S_{H_2S}$ ranges from −0.7‰ to 1.8‰ (Table 4). These $\delta^{34}S_{H_2S}$ values are similar to but slightly depleted in ^{34}S relative to estimated means ($\delta^{34}S_{H_2S}$ from 1.8‰ to 3.0‰) for sulfides from the older pre-Main Stage. We consider three possible origins for sulfur in the younger sulfides.

In the Main Stage, magmatic–hydrothermal fluids with bulk $\delta^{34}S_{\Sigma S}$~10‰ depressurize, undergo brine–vapor unmixing, and H_2S loss as well as reduction of SO_4^{2-} to H_2S. Sulfides are precipitated from brine as well as from condensates having the H_2S-rich vapor. These processes cause the $X_{SO_4^{2-}}$ to decrease with decreasing temperature from initial ratios of ~0.75 to 0.50 and possibly as little as 0.33 by ~200 °C (SO_4^{2-}/H_2S~1:2). Sample MMM2236M contains barite (27.3‰) and pyrite (1.3‰) deposited in the vuggy center of a late Main Stage vein, and this mineral pair yields a sulfur isotopic temperature of 215 °C (Table 5). Assuming a composition of $\delta^{34}S_{\Sigma S}$~10‰ for bulk sulfur, the $X_{SO_4^{2-}}$ would be about 0.4. As noted below, such a $X_{SO_4^{2-}}$ value could not represent equilibrium with a Main Stage fluid, and instead would reflect the slow kinetics of sulfide–sulfate reactions at <350 °C (cf. Ohmoto and Rye, 1979). Thus, the entire suite of sulfides at Butte could be deposited from a fluid with one parental composition of $\delta^{34}S$~10‰ (Fig. 7). However, it should be noted that low-pH conditions that produce Main Stage-like advanced argillic and white sericitic alteration in many high-sulfidation and

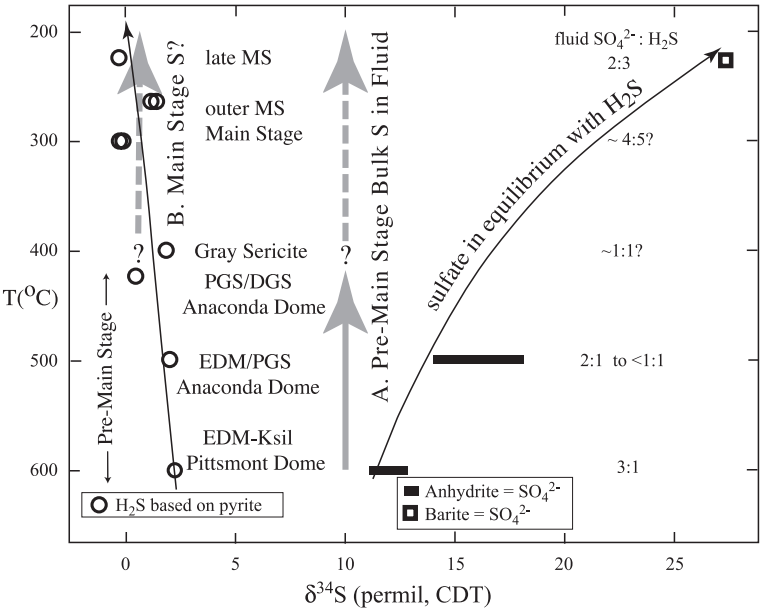

Fig. 7. Compositions of H_2S and SO_4^{2-} in hydrothermal fluids as a function of alteration stage and temperature (decreasing with younger age) from the mineral isotopic data of Table 4. Thin black arrows illustrate trends of H_2S and corresponding SO_4^{2-} calculated to be in equilibrium. Note that sulfate from the K-silicate (early dark mica/pale gray sericitic) assemblage from the Anaconda Dome plots to the right of the SO_4^{2-}, consistent with vapor separation and sulfur isotopic fractionation (see text). Thick lines are possible bulk sulfur ($\delta^{34}S_{\Sigma S}$) compositions of the hydrothermal fluids. For line A, magmatic sulfur with $\delta^{34}S$=10‰ could produce pre-Main Stage and Main Stage sulfide and sulfate $\delta^{34}S$ values as observed and yield the molar SO_4^{2-}/H_2S ratios shown to the right. For line B, gray-sericitic and Main Stage sulfur is assumed to be dominated by H_2S and requires input of a second batch of sulfur with $\delta^{34}S \approx 1$‰.

Table 5
Oxygen and sulfur isotope data for a subset of pre-Main Stage (anhydrite) and Main Stage (barite) sulfate samples at Butte

Stage/sample/ mineral		$\delta^{18}O$ (‰, SMOW)	$\delta^{34}S$ (‰, CDT)	T, °C	$\delta^{18}O$ (‰, H_2O)
Main Stage					
MMM2236M	Brt	12.4	27.3	215	6.6
DUDAS 3	Brt	10.5	18.6	345?	4.7
GRL 9274	Brt	8.3	13.5	480?	2.5
GRL 3183	Brt	−0.3	4.4	1270?	−6.1
Pre-Main Stage, Anaconda Dome					
Bu-8a	Anh	9.5	18.2	370	6.5
Bu-8b	Anh	9.0	18.1	360	5.7
Bu-9a	Anh	8.1	14.7	460	6.9
Pittsmont Dome (DDH-10)					
11172-2262.5	Anh	7.4	11.2	640	8.3
11172-2264.5	Anh	7.0	12.2	555	7.0
11172-2460.5	Anh	7.2	9.8	560	7.3
11172-3252.5	Anh	7.9	12.3	555	7.9
11172-3429.5	Anh	7.4	12.7	480	6.5
11172-4208	Anh	8.2	12.6	545	8.1
Means		7.5		555	7.5
11172-2934	Qtz	9.6		550	7.7
11172-3920	Qtz	8.9		550	7.0
11172-4166	Qtz	9.5		550	7.6
Bu 96018	Qtz	10.0		550	8.1
Means		9.5		550	7.6
Quartz ^{18}O temperature from $\Delta_{Qtz-Anh}$=585 °C					

Temperatures for sulfate samples based on sulfate–sulfide isotopic equilibria. Data for quartz and assumed temperatures from Zhang (2000). Calculated $\delta^{18}O$ compositions of water equilibrating with anhydrite, barite, and quartz based on fractionation equations of Chiba et al. (1981), Friedman and O'Neil (1977), and Matsuhisa et al. (1979), respectively. The calculations for water equilibrating with all four barite samples assume a depositional temperature of 215 °C.

low-pH epithermal systems augment sulfate–sulfide equilibrium at temperatures of <350 °C (Rye et al., 1992).

Alternatively, under equilibrium conditions at 200 to 350 °C, the Main Stage should be characterized by relatively high H_2S/SO_4^{2-} (>100, or $X_{SO_4^{2-}} \leq 0.01$), as is consistent with the low-pH alteration (kaolinite–'sericite') and high-sulfidation assemblages (pyrite+ bornite) (Ohmoto and Rye, 1979). In this case, the isotopic composition of H_2S must represent the $\delta^{34}S_{\Sigma S}$ composition of the fluid. Therefore, the Main Stage $\delta^{34}S_{H_2S}$, which ranges from −0.3‰ to 1.4‰ on the basis of the mean compositions of pyrite (Table 4), would be equivalent to bulk-sulfur $\delta^{34}S_{\Sigma S}$ of ~0.5‰, which is distinctly lighter than the ~10‰ inferred for pre-Main Stage sulfur, as portrayed in Fig. 7.

A third possibility, which we discount as unlikely, is that sulfur was remobilized from the earlier pre-Main Stage 'early dark micaceous' and K-silicate assemblages into the later 'gray-sericitic' or Main Stage mineral zones and assemblages. Brimhall (1979, 1980) demonstrated via geological relations and assays that Cu was locally removed from pre-Main Stage zones in the selvages of younger cross-cutting Main Stage veins. Brimhall proposed that the leached Cu was added to the Main Stage veins. The case for the leaching of sulfur cannot be easily made, but had it occurred, the process would have involved only the leaching of pre-Main Stage sulfide–sulfur and its redeposition as Main Stage sulfur (all with $\delta^{34}S_{H_2S}$ ~0 to 3‰). On geological grounds, this process is not likely because both the 'gray-sericitic' and Main Stage selvages have higher sulfide–mineral contents than the older pre-Main Stage zones; hence, there is direct evidence for addition rather than removal of sulfur. Second, all Main Stage veins and selvages lack anhydrite and contain only rare amounts sulfates, which indicate that Main Stage fluids removed anhydrite and sulfate from the older pre-Main Stage zones. There is no isotopic evidence that isotopically heavy sulfate ($\delta^{34}S_{SO_4^{2-}}$~13‰) was introduced, reduced, and deposited as metallic sulfides at <350 °C by the Main Stage fluids. Such a process would be expected to produce either isotopically light sulfide minerals under conditions of minor (<10%) equilibrium reduction/reaction, or isotopically heavy sulfide minerals under >50% equilibrium reduction or any amount of non-equilibrium reduction. The relatively small variations in the mean $\delta^{34}S_{H_2S}$ values of 'gray-sericitic' and Main Stage assemblages indicate a relatively uniform fluid composition and argue persuasively against significant amounts of sulfate reduction or sulfate–sulfide equilibrium.

Pyrite of the 'gray-sericitic' assemblage yields a mean calculated $\delta^{34}S_{H_2S}$ of 1.8‰ (Table 4), and could have formed by either of the above mechanisms, depending on SO_4^{2-}/H_2S of the causative hydrothermal fluids. Minerals formed by these fluids have magmatic–hydrothermal oxygen- and hydrogen-isotope compositions (Zhang, 2000), and were trapped at 400 to 425 °C according to fluid-inclusion data (Rusk, 2003). Sulfate is not present in the pyrite–

quartz veinlets or selvages, but the veinlets contain up to 5 vol.% void space that may represent sites of former, subsequently leached anhydrite.

Without having better estimates of the $X_{SO_4^{2-}}$ and the $\delta^{34}S$ of any SO_4^{2-} in the fluids that formed the 'gray-sericitic' and Main Stage assemblages, we cannot determine the $\delta^{34}S_{\Sigma S}$ compositions of the fluids. The fluids could represent a similar ~10‰ sulfur source as the pre-Main Stage K-silicate magmatic–hydrothermal fluids, provided that H_2S and SO_4^{2-} did not equilibrate below ~400 °C. Alternatively, the fluids could represent a distinctly different source with $\delta^{34}S$ of ~0 to 2‰ and dominated by H_2S as summarized by Fig. 7.

6.2.8. Origin of sulfur in late Main Stage barite

There is both mineralogical and isotopic evidence to support the postulated requirements of low $X_{SO_4^{2-}}$ and limited sulfate–sulfide equilibration. First, anhydrite is absent and alunite and barite are present only as trace minerals in these later assemblages (Meyer et al., 1968), and the sulfides reported by Lange and Cheney (1971) and Lange and Krouse (1984) do not reveal any isotopic evidence for having inherited via equilibration heavy sulfate–sulfur from remobilized anhydrite. Second, barite is one of the last minerals to have formed during Main Stage mineralization, and only one of the four samples (MMM2236M in Table 1) contains ^{34}S-enriched sulfate (27.3‰) that indicates isotopic equilibration as a hypogene component at realistic hydrothermal temperatures (215 °C). This enrichment relative to associated pyrite (1.3‰) suggests that sulfate at the time of deposition was a minor fraction ($X_{SO_4^{2-}} \leq 0.10$) of total sulfur in the system, or that limited cations (i.e., Ba, Pb) were available to precipitate sulfate because of the retrograde solubility of anhydrite. Third, barite of the other three samples exhibits unusually variable ^{34}S depletion (18.6‰, 13.5‰, and 4.4‰) relative to the heavy sulfate and near-constant $\delta^{34}S$ in associated pyrite (2.2‰, 2.3‰, and 1.3‰). Collectively, these features are evidence of increasing isotopic disequilibrium that accompanied incorporation of progressively larger quantities of type-b sulfate. Type-b sulfates, as defined by Ohmoto (1986) and Ohmoto and Goldhaber (1997), may form by oxidation of H_2S without isotopic equilibration in the hydrothermal fluid, and they inherit the ^{34}S-depleted signature of their reduced precursor. The source of most sulfate–sulfur in Butte barite presumably was from the oxidation of H_2S ($\delta^{34}S \approx 1‰$ to 2‰). Oxygen isotopic data, described in the next section, intimate that oxygenated meteoric waters caused this oxidation. The ^{34}S-enriched barite (27.3‰) and all pre-Main Stage anhydrite previously discussed are considered to be type-a sulfates formed in isotopic equilibrium with sulfide.

6.3. Oxygen-isotope composition of sulfates

Means and ranges of $\delta^{18}O$ data for anhydrite of the Pittsmont Dome (six samples; 7.0‰ to 8.2‰) and Anaconda Dome (three samples; 8.1‰ to 9.5‰), and for barite of the Main Stage veins (four samples; −0.3‰ to 12.4‰) constitute three distinct populations. Moreover, the tabulated isotopic data for oxygen and sulfur (Table 5) suggest a near-perfect covariant relationship in a plot of $\delta^{18}O$ versus $\delta^{34}S$ (Fig. 8). This trend is interpreted to have resulted largely from temperature-induced fractionation for anhydrite of the pre-Main Stage K-silicate assemblage, and perhaps only partly for one or two of the ^{34}S-enriched samples of the Main Stage barite. Much or most of the similar trend for barite, especially for the ^{34}S-depleted samples, is thought to be accidental and the result of contamination by unequilibrated type-b sulfate derived from isotopically light H_2S.

Zhang (2000) reported $\delta^{18}O$ values for quartz in four samples of K-silicate alteration from the Continental mine area of the Pittsmont Dome. Three of the four samples are from the same interval of DDH 10 from which the samples of anhydrite were collected (Table 5). The $\delta^{18}O$ values of quartz are invariably heavier than those of anhydrite, a feature consistent with the established fractionations for these minerals. The delta value of 2.0‰, obtained from the difference between mean $\delta^{18}O$ values of quartz (9.5‰) and anhydrite (7.5‰), and applied to the quartz–anhydrite fractionation equation as derived from those for quartz–H_2O (Matsuhisa et al., 1979) and anhydrite–H_2O (Chiba et al., 1981), provides a mean temperature estimate of 584 °C for oxygen-isotope equilibration. This temperature is similar to and apparently corroborative of the mean estimate of 556 °C determined independently from the $\delta^{34}S$ data for these sulfate–sulfide pairs (Table 5).

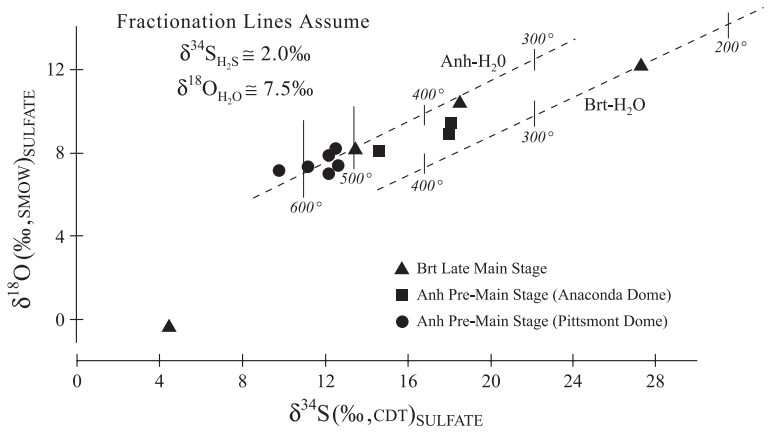

Fig. 8. Plot of $\delta^{18}O$ versus $\delta^{34}S$‰ values for anhydrite (Anh) of the pre-Main Stage K-silicate assemblage from the Pittsmont and Anaconda domes, and for late barite (Brt) of the Main Stage veins. Linearity of the pre-Main Stage anhydrite data suggests a dominantly temperature-induced fractional trend, whereas that of the Main Stage barite data is likely accidental and an artifact of mixing at low temperatures with ^{18}O-depleted meteoric waters and ^{34}S-depleted H_2S sulfide–sulfur.

The $\delta^{18}O$ compositions of Butte hydrothermal fluids can be calculated from the $\delta^{18}O$ values of barite, anhydrite, and quartz and the estimated temperatures of formation shown in Table 5 using the fractionation factors of Matsuhisa et al. (1979) and Chiba et al. (1981). The $\delta^{18}O$ values for waters equilibrating with anhydrite of the Pittsmont and Anaconda domes range from 6.5‰ to 8.3‰, and 5.7‰ to 6.9‰, respectively, and those for quartz in the associated K-silicate assemblage of the Pittsmont Dome range from 7.0‰ to 8.1‰ (Table 5). The $\delta^{18}O$ values of magmatic waters generally range from 5.5‰ to 10‰ (Taylor, 1997). Thus, all calculated values of $\delta^{18}O$ for anhydrite and quartz of the pre-Main Stage K-silicate assemblage are presumed from the isotopic criteria to be representative of magmatic waters.

In contrast, the $\delta^{18}O$ values for fluids that precipitated the late barite in Main Stage veins range markedly from −6.1‰ to 6.6‰. Barite sample MMM2236M has the heaviest sulfate $\delta^{34}S$ (27.3‰), heaviest sulfate $\delta^{18}O$ (12.4‰), and heaviest calculated fluid $\delta^{18}O$ (6.6‰), collectively suggesting deposition from a predominantly magmatic fluid. However, the other three barite samples exhibit variably smaller mineral–sulfate $\delta^{34}S$ values (18.6‰ to 4.4‰), mineral–sulfate $\delta^{18}O$ values (10.5‰ to −0.3‰), and calculated $\delta^{18}O$ values (4.7‰ to −6.1‰) for the barite-depositing fluids. These isotopic trends are unusual. The decreasing $\delta^{18}O$ values of barite and its calculated depositional fluids during late Main Stage mineralization suggest an influx of ^{18}O-depleted meteoric waters into a Butte hydrothermal system originally dominated by magmatic waters of a more ^{18}O-enriched (5.5‰ to 10‰) composition. The oxygen and hydrogen isotopic data on Main Stage mica and clay also indicate meteoric water influx (Sheppard and Taylor, 1974). Incursion of these oxygenated meteoric waters resulted in the oxidation of an unknown quantity of H_2S ($\delta^{34}S \approx 1‰$ to 2‰) to type-b sulfate that mixed with variable amounts of coexisting hypogene SO_4^{2-} ($\delta^{34}S \geq 27‰$) without isotopic equilibration to form barite having relatively depleted $\delta^{34}S$ values of 4.4‰ or less.

7. Conclusions

The pre-Main Stage hydrothermal system at Butte represents a relatively deep (~7 km depth) porphyry Cu–Mo deposit upon which the younger polymetallic base-metal veins of the Main Stage were superimposed. Pre-Main Stage hydrothermal mineralization produced K-silicate alteration, ‘early dark mica’ veinlets, and sulfur-bearing minerals dominated by anhydrite, pyrite, chalcopyrite, and molybdenite. The eastern Pittsmont Dome center represents a simple system in which fluid inclusions were trapped as a single-phase fluid of low salinity (Rusk, 2003), and the $\delta^{34}S_{\Sigma S}$ of both the hydrothermal fluid and parent magma may be estimated. The observed anhydrite–

pyrite fractionation indicates deposition and isotopic equilibrium at ~550–600 °C, in accord with petrological estimates. The isotopic data and a variety of geochemical arguments indicate that the hydrothermal fluids at these temperatures were sulfate-rich ($X_{SO_4^{2-}}$ of ~0.70 to 0.75). This high ratio of sulfate/sulfide is consistent with magmatic gases having $SO_2 \gg H_2S$ as a consequence of strongly oxidized conditions in the granitic melt from which the fluids were derived. The $\delta^{34}S_{\Sigma S}$ of this pre-Main Stage system is inferred to have been ~9.9‰ and represents the most ^{34}S-enriched porphyry hydrothermal system of which we are aware. The elevated $\delta^{34}S$ of the parental Butte quartz porphyry magmas is attributed to incorporation of isotopically heavy evaporite sulfate (>50% of the magmatic sulfur) that was probably derived mainly from the sedimentary rocks of the Proterozoic Belt Supergroup, which was intruded by the host Boulder batholith.

In pre-Main Stage ores of the western Anaconda Dome center, anhydrite is ^{34}S-enriched relative to that of the Pittsmont Dome, whereas $\delta^{34}S$ values for pyrite are similar. We attribute this ^{34}S-enrichment of sulfate to brine–vapor unmixing and Rayleigh fractionation via escape of a ^{34}S-depleted H_2S-rich vapor phase, a process that is consistent with the presence of both brine and vapor-rich fluid inclusions. Numerical modeling suggests that a 10‰ to 50% sulfur loss in this manner may produce the ^{34}S-enriched anhydrite values precipitated from the Anaconda brine. Sulfate reduction to H_2S in the brine is a required part of the unmixing, and can be generally correlated with deposition of magnetite, pyrite, and chalcopyrite, and with acidic alteration. Wide ranges of anhydrite isotopic compositions, which are also observed at the Galore Creek (British Columbia) and El Salvador (Chile) porphyry-Cu deposits, may be associated with brine–vapor unmixing. Our hypothesis may be widely applicable to other porphyry systems.

Evolution of sulfur in the later pre-Main Stage 'gray-sericitic' and younger Main Stage systems remains incompletely understood. Isotopic results, including data for barite–pyrite pairs and comparisons of Main Stage pyrite to sulfate leached from the pre-Main Stage by the younger fluids, indicate that sulfate–sulfide isotopic equilibrium was generally incomplete or absent. The ratio of sulfate/sulfide in the fluids cannot be directly estimated because of the paucity of sulfates and attendant isotopic data. One interpretation of the data is that sulfate/sulfide equilibrium was lacking at <350 °C, and therefore the fluids remained relatively sulfate-rich ($X_{SO_4^{2-}}$ of ~0.33–0.50). Thus, Main Stage sulfides could have precipitated from the same ~10‰ magmatic–hydrothermal parent, and a single sulfur isotopic reservoir would characterize the entire Butte system. Alternatively, if only partial sulfate/sulfide equilibrium was attained at <350 °C, so that fluids became relatively H_2S-rich ($X_{SO_4^{2-}} \leq 0.1$), then a second fluid with a distinctly different and lighter $\delta^{34}S_{\Sigma S} \approx \delta^{34}S_{H_2S} \approx$ 0.5‰ to 2‰) is required for the Main Stage and also possibly for the earlier 'gray-sericitic' hydrothermal systems. The $\delta^{18}O$ compositions of late Main Stage barite suggest that little sulfide–sulfate equilibrium prevailed, and the compositions support the proposition of mixing of meteoric and magmatic water components.

Acknowledgments

This project was supported largely by the National Science Foundation through grants EAR-9600054 (Dilles and Field) and EAR-9704280 (Reed). We thank Montana Resources for permission to log and sample core, and thank the Montana Bureau of Mines and Geology for access to the Anaconda (Geologic Research Laboratory) sample collection. We especially appreciate the persistent and successful efforts of Lester Zeihen to preserve the Anaconda sample collection. Robert A. Houston and Brian G. Rusk provided important contributions to the mapping and compilation of Butte geology and to the study of fluid inclusions and vein petrology, respectively. The timely assistance of Cynthia L. Kester of the U.S. Geological Survey (Denver) in providing the $\delta^{18}O$ analyses of our sulfates is gratefully acknowledged. **[PD]**

References

Ames, R.L., 1962. Sulfur isotopic study of the Tintic Mining District, Utah. PhD thesis, Yale University, New Haven, Connecticut.

Bachinski, D.J., 1969. Bond strength and sulfur isotopic fractionation in coexisting sulfides. Econ. Geol. 64, 56–65.

Barton, P.B., Skinner, B.J., 1979. Sulfide mineral stabilities. In: Barnes, H.L. (Ed.), Geochemistry of Hydrothermal Ore Deposits, (2nd ed.)Wiley, New York, pp. 278–403.

Becraft, G.E., Pickney, D.M., Rosenblum, S., 1963. Geology and mineral deposits of Jefferson City quadrangle, Jefferson and Lewis and Clark counties, Montana. U. S. Geol. Surv. Prof. Pap. 428.

Blatt, H., Middleton, G., Murray, R., 1980. Origin of Sedimentary Rocks. Prentice-Hall, Englewood Cliffs, NJ.

Bodnar, R.J., Burnham, C.W., Sterner, S.M., 1985. Synthetic fluid inclusions in natural quartz: III. Determination of phase equilibrium properties in the system H_2O–NaCl to 1000 °C and 1500 bars. Geochim. Cosmochim. Acta 49, 1871–1873.

Borrok, D., Kesler, S.E., Vogel, T.A., 1999. Sulfide minerals in intrusive and volcanic rocks of the Bingham-Park City Belt, Utah. Econ. Geol. 94, 1213–1230.

Brimhall Jr., G.H., 1977. Early fracture-controlled disseminated mineralization at Butte, Montana. Econ. Geol. 72, 37–59.

Brimhall Jr., G.H., 1979. Lithologic determination of mass-transfer mechanism of multiple-stage porphyry copper mineralization at Butte, Montana: vein formation by hypogene leaching and enrichment of potassium silicate protore. Econ. Geol. 74, 556–589.

Brimhall Jr., G.H., 1980. Deep hypogene oxidation of porphyry copper potassium-silicate protore at Butte, Montana: a theoretical evaluation of the copper mobilization hypothesis. Econ. Geol. 75, 384–409.

Brimhall, G.H., Agee, C., Stoffregen, R., 1985. The hydrothermal conversion of hornblende to biotite. Can. Mineral. 23, 369–379.

Brownlow, A.H., Kurz, S.L., 1979. Occurrence, distribution, and composition of sulfide minerals, Boulder batholith, Montana. Miner. Depos. 14, 175–184.

Burnham, C.W., 1997. Magma and hydrothermal fluids. In: Barnes, H.L. (Ed.), Geochemistry of Hydrothermal Ore Deposits, (3rd ed.)Wiley, New York, pp. 71–136.

Carroll, M.R., Webster, J.D., 1994. Solubilities of sulfur, noble gases, nitrogen, chlorine, and fluorine in magmas. In: Carroll, M.R., Holloway, J.R. (Eds.), Volatiles in Magmas, Rev. Mineral., vol. 30, pp. 231–280.

Chandler, F.W., Gregoire, D.C., 2000. Sulphur, strontium and boron isotopes from replaced sulphate evaporite nodules in the Altyn Formation, Lower Belt Supergroup, Montana: clues to the sedimentary environment of the Sullivan deposit. In: Lydon, J.W., Hoy, T., Slack, J.F., Knapp, M.E. (Eds.), The Geological Environment of the Sullivan Deposit, British Columbia, Spec. Publ.-Geol. Assoc. Can. Miner. Depos. Div. vol. 1, pp. 251–258.

Chiba, H., Kusakabe, M., Hirano, S.-I., Matsuo, S., Somiya, S., 1981. Oxygen isotope fractionation factors between anhydrite and water from 100 to 500° C. Earth Planet. Sci. Lett. 53, 55–62.

Claypool, G.E., Holser, W.T., Kaplan, I.R., Sakai, H., Zak, I., 1980. The age curves of sulfur and oxygen isotopes in marine sulfate and their mutual interpretation. Chem. Geol. 28, 199–260.

Dilles, J.H., 1987. Petrology of the Yerington Batholith, Nevada: evidence for evolution of porphyry copper ore fluids. Econ. Geol. 82, 1750–1789.

Dilles, J.H., Field, C.W., 1996. Sulfur geochemistry of porphyry copper deposits as a record of magma degassing: data from the Yerington district, Nevada. Abstr. Programs-Geol. Soc. Am. 28 (7), A93.

Dilles, J.H., Reed, M.H., Roberts, S., Zhang, L., Houston, R., 1999. Early magmatic–hydrothermal features related to porphyry copper mineralization at Butte, Montana. Abstr. Programs-Geol. Soc. Am. 31 (7), A380.

Ehlers, E.G., Blatt, H., 1982. Petrology; Igneous, Sedimentary, and Metamorphic. W.H. Freeman, San Francisco.

Farquhar, G.D., Henry, B.K., Styles, J.M., 1997. A rapid on-line technique for determination of oxygen isotope composition of nitrogen-containing organic matter and water. Rapid Commun. Mass Spectrom. 11, 1554–1560.

Field, C.W., 1966. Sulfur isotope abundance data, Bingham District, Utah. Econ. Geol. 61, 850–871.

Field, C.W., Gustafson, L.B., 1976. Sulfur isotopes in the porphyry copper deposit at El Salvador, Chile. Econ. Geol. 71, 1533–1548.

Field, C.W., Rye, R.O., Dymond, J.R., Whelan, J.F., Senechal, R.G., 1983. Metalliferous sediments of the East Pacific. In: Shanks III, W.C. (Ed.), Cameron Volume on Unconventional Mineral Deposits. Soc. Mining Eng. Am. Inst. Mining Metall. Petroleum Eng, pp. 133–156.

Field, C.W., Sakai, H., Ueda, A., 1984. Isotopic constraints on the origin of sulfur in oceanic igneous rocks. In: Wauschkuhn, A., Kluth, C., Zimmermann, R.A. (Eds.), Syngenesis and Epigenesis in the Formation of Mineral Deposits. Springer-Verlag, Berlin, pp. 573–589.

Field, C.W., Rye, R.O., Dilles, J.H., Gustafson, L.B., 2000. Sulfur isotope abundances of hypogene sulfate–sulfide assemblages in porphyry-type deposits of the American Cordillera. Abstr. Programs-Geol. Soc. Am. 32 (7), A48.

Friedman, I., O'Neil, J.R., 1977. Compilation of stable isotope fractionation factors of geochemical interest. In: Fleischer, M. (Ed.), Data of Geochemistry, (6th ed.). U. S. Geol. Surv. Prof. Pap., vol. 440-KK, pp. KK1–KK12.

Harrison, J.E., 1972. Precambrian Belt basin of northwestern United States: its geometry, sedimentation, and copper occurrences. Geol. Soc. Amer. Bull. 83, 1215–1240.

Hayes, T.S., Einaudi, M.T., 1986. Genesis of the Spar Lake strata-bound copper–silver deposit, Montana: part I. Controls inherited from sedimentation and diagenesis. Econ. Geol. 81, 1899–1931.

Hayes, T.S., Rye, R.O., Whelan, J.F., Landis, G.P., 1989. Geology and sulphur-isotope geothermometry of the Spar Lake strata-bound Cu–Ag deposit in the Belt Supergroup, Montana. In: Boyle, R.W., Brown, A.C., Jowett, E.C., Kirkham, R.V. (Eds.), Sediment-Hosted Stratabound Copper Deposits, Spec. Pap.-Geol. Assoc. Can., vol. 36, pp. 319–338.

Hedenquist, J.W., Lowenstern, J.B., 1994. The role of magmas in the formation of hydrothermal ore deposits. Nature 370, 519–526.

Hemley, J.J., Cygan, G.L., Fein, J.B., Robinson, G.R., D'Angelo, W.M., 1992. Hydrothermal ore-forming processes in light of studies in rock-buffered systems: I. Iron–copper–zinc–lead sulfide solubilities. Econ. Geol. 87, 1–22.

Holland, H.D., Malinin, S.D., 1979. The solubility and occurrence of non-ore minerals. In: Barnes, H.L. (Ed.), Geochemistry of Hydrothermal Ore Deposits, (2nd ed.)Wiley, New York, pp. 461–508.

Houston, R.A., 2001. Geology and structural history of the Butte District, Montana. Corvallis, Oregon. MSc thesis, Oregon State University, Corvallis, Oregon.

Jensen, M.L., 1959. Sulfur isotopes and hydrothermal mineral deposits. Econ. Geol. 54, 374–394.

Johnson, J.W., Oelkers, E.H., Helgeson, H.C., 1992. SUPCRT92: a software package for calculating the standard thermodynamic properties of minerals, gases, aqueous species, and reactions fro 1 to 5000 bars and 0° to 1000 °C. Comput. Geosci. 9, 899–947.

Kiyosu, Y., Kurahashi, M., 1983. Origin of sulfur species in acid sulfate–chloride thermal waters, northeastern Japan. Geochim. Cosmochim. Acta 47, 1237–1245.

Klepper, M.R., Weeks, R.A., Ruppel, E.T., 1957. Geology of the southern Elkhorn Mountains, Montana. U. S. Geol. Surv. Prof., 292.

Kusakabe, M., Nakagawa, S., Hori, S., Matsuhisa, Y., Ojeda, J.M., Serrano, L., 1984. Oxygen and sulfur isotopic compositions of quartz, anhydrite, and sulfide minerals from the El Teniente and Rio Blanco porphyry copper deposits, Chile. Bull.-Geol. Surv. Japan 35, 583–614.

Lange, I.M., Cheney, E.S., 1971. Sulfur isotope reconnaissance of Butte, Montana. Econ. Geol. 66, 63–74.

Lange, I.M., Krouse, H.R., 1984. Sulfur isotopic variations in the A2844 vein and wall rock, Butte, Montana. Geochem. J. (Japan) 18, 269–280.

Long, K.R., 1995. Production and reserves of Cordilleran (Alaska to Chile) porphyry copper deposits. In: Pierce, F.W., Bolm, J.G. (Eds.), Porphyry Copper Deposits of the American Cordillera, Ariz. Geol. Soc. Dig., vol. 20, pp. 35–68.

Lund, K., Aleinikoff, J.N., Kunk, M.J., Unruh, D.M., Zeihen, G.D., Hodges, W.C., du Bray, E.A., O'Neill, J.M., 2002. SHRIMP U–Pb and $^{40}Ar/^{39}Ar$ age constraints for relating plutonism and mineralization in the Boulder Batholith region, Montana. Econ. Geol. 97, 241–267.

Lyons, T.W., Luepke, J.L., Schreiber, M.E., Zieg, G.A., 2000. Sulfur geochemical constraints on Mesoproterozoic restricted marine deposition: Lower Belt Supergroup, northwestern United States. Geochim. Cosmochim. Acta 64, 427–437.

Mandeville, C.W., Carey, S., Sigurdsson, H., 1996. Magma mixing, fractional crystallization and volatile degassing during the 1883 eruption of Krakatau Volcano, Indonesia. J. Volcanol. Geotherm. Res. 74, 243–274.

Martin, M.W., Dilles, J.D., 2000. Timing and duration of the Butte porphyry Cu–Mo system. Abstr. Programs-Geol. Soc. Am. 32 (6), A28.

Martin, M.W., Dilles, J.H., Proffett, J.M., 1999. U–Pb geochronologic constraints for the Butte porphyry system. Abstr. Programs-Geol. Soc. Am. 31 (7), A380–A381.

Matsuhisa, Y., Goldsmith, J.R., Clayton, R.N., 1979. Oxygen isotopic fractionation in the system quartz–albite–anorthite–water. Geochim. Cosmochim. Acta 43, 1131–1140.

Meyer, C., 1965. An early potassic type of wall-rock alteration at Butte, Montana. Am. Mineral. 50, 1717–1722.

Meyer, C., Hemley, J.J., 1967. Wall rock alteration. In: Barnes, H.L. (Ed.), Geochemistry of Hydrothermal Ore Deposits. Wiley, New York, pp. 166–235.

Meyer, C., Shea, E.P, Goddard Jr., C.C., and Staff, 1968. Ore deposit at Butte, Montana. Ore Deposits of the United States 1933/1967, the Graton-Sales Volume (Vol. II). Am. Inst. Mining Metall. Petroleum Eng., New York, pp. 1373–1416.

Newhouse, W.H., 1936. Opaque oxides and sulphides in common igneous rocks. Geol. Soc. Amer. Bull. 47, 1–52.

Ohmoto, H., 1972. Systematics of sulfur and carbon isotopes in hydrothermal ore deposits. Econ. Geol. 67, 551–578.

Ohmoto, H., 1986. Stable isotope geochemistry of ore deposits. In: Valley, J.W., Taylor Jr., H.P., O'Neil, J.R. (Eds.), Stable Isotopes in High Temperature Geological Processes, Rev. Mineral., vol. 16, pp. 491–559.

Ohmoto, H., Goldhaber, M.B., 1997. Sulfur and carbon isotopes. In: Barnes, H.L. (Ed.), Geochemistry of Hydrothermal Ore Deposits, (3rd ed.)Wiley, New York, pp. 517–611.

Ohmoto, H., Lasaga, A.C., 1982. Kinetics of reactions between aqueous sulfates and sulfides in hydrothermal systems. Geochim. Cosmochim. Acta 46, 1727–1745.

Ohmoto, H., Rye, R.O., 1979. Isotopes of sulfur and carbon. In: Barnes, H.L. (Ed.), Geochemistry of Hydrothermal Ore Deposits, (2nd ed.)Wiley, New York, pp. 509–567.

O'Neill, J.M., 1995. Table Mountain Quartzite and Moose Formation (new names) and associated rocks of the Middle Proterozoic Belt Supergroup, Highland Mountains, southwestern Montana. U.S. Geol. Surv. Bull. 2121-A, 26 p.

Page, R.H., 1979. Alteration–mineralization history of the Butte, Montana, ore deposit, and transmission electron microscopy of phyllosilicate alteration phases. PhD thesis, University of California, Berkeley.

Proffett, J.M., 1973. Structure of the Butte district, Montana. In: Miller, R.N. (Ed.), Soc. Econ. Geol. Butte Field Meeting Guidebook. The Anaconda, pp. G1–G12.

Reed, M.H., 1979. Butte District Early Stage Geology. Anaconda Report 40, 24 pp., plates and figures.

Reed, M.H., 1980. Distribution of Mineralization at Butte. Anaconda Report 25, 17 pp., lates and figures.

Reed, M.H., 1999. Zoning of metals and early potassic and sericitic hydrothermal alteration in the Butte, Montana, porphyry Cu–Mo deposit. Abstr. Programs-Geol. Soc. Am. 31 (7), A381.

Rieder, M., Cavazzini, G., D'Yakonov, Y.S., Frank-Kamenetskii, V.A., Gottardi, G., Guggenheim, S., Koval, P.V., Müller, G., Neiva, A.M.R., Radoslovich, E.W., Robert, J.-L., Sassi, F.P., Takeda, H., Weiss, Z., Wones, D.R., 1998. Nomenclature of the micas. Can. Mineral. 36, 905–912.

Roberts, S.A., 1973. Pervasive early alteration in the Butte district, Montana. In: Miller, R.N. (Ed.), Soc. Econ. Geol. Butte Field Meeting Guidebook. Anaconda, pp. HH1–HH8.

Roberts, S.A, 1975. Early hydrothermal alteration and mineralization in Butte district, Montana. PhD thesis, Harvard University Cambridge, Massachusetts.

Robson, J., 1971. An optical study of the magmatic rocks near Butte, Montana. MSc thesis, Montana School of Mines, Butte, Montana.

Ruppel, E.T., 1963. Geology of the Basin quadrangle, Jefferson, Lewis and Clark and Powell counties, Montana. U. S. Geol. Surv. 1151, 121 p.

Rusk, B.G., 2003. Cathodoluminescent quartz textures and fluid inclusions in veins of the porphyry copper–molybdenum deposit in Butte, Montana: constraints on the physical and chemical evolution of the hydrothermal system. PhD thesis, University of Oregon, Eugene.

Rusk, B., Reed, M., 2002. Scanning electron microscope–cathodoluminescence analysis of quartz reveals complex growth histories in veins from the Butte porphyry copper deposit, Montana. Geology 30, 727–730.

Rusk, B., Reed, M.H., Dilles, J.H., 1999. Fluid inclusions in barren quartz and quartz–molybdenite veins in the porphyry Cu–Mo deposits, Butte, Montana. Program Abstr.-Geol. Soc. Am. 31 (7), A381.

Rusk, B., Reed, M., Dilles, J., Bodnar, R.J., 2000. Magmatic fluid evolution from an ancient magmatic–hydrothermal system; the porphyry copper–molybdenum deposit, Butte, MT. Abstr. Programs-Geol. Soc. Am. 32 (7), A112.

Rusk, B.G., Reed, M.H., Dilles, J.H., 2002. Fluid inclusion evidence for evolution of hydrothermal fluids from the porphyry copper deposit in Butte, MT. Abstr. Programs-Geol. Soc. Am. 34 (6), 337.

Rusk, B., Reed, M.H., Dilles, J.H., Klemm, L., Heinrich, C., 2004. Compositions of magmatic hydrothermal fluids determined by LA-ICP-MS of fluid inclusions from the porphyry copper–molybdenum deposit at Butte, Montana. Chem. Geol. 210, 173–199.

Rye, R.O., Bethke, P.M., Wasserman, M.D., 1992. The stable isotope geochemistry of acid sulfate alteration. Econ. Geol. 87, 225–262.

Sakai, H., 1968. Isotopic properties of sulfur compounds in hydrothermal processes. Geochem. J. (Japan) 2, 29–49.

Sakai, H., Casadevall, T.J., Moore, J.G., 1982. Chemistry and isotope ratios of sulfur in basalts and volcanic gases at Kilauea Volcano, Hawaii. Geochim. Cosmochim. Acta 46, 729–738.

Sales, R.H., 1914. Ore deposits at Butte, Montana. Am. Inst. Min. Metall. Pet. Eng. Trans. 46, 3–106.

Sales, R.H., Meyer, C., 1948. Wall rock alteration, Butte, Montana. Am. Inst. Min. Metall. Pet. Eng. Trans. 178, 9–35.

Sales, R.H., Meyer, C., 1951. Effect of post-ore dike intrusion on Butte ore minerals. Econ. Geol. 46, 813–820.

Sasaki, A., Arikawa, Y., Folinsbee, R.E., 1979. Kiba reagent method of sulfur extraction applied to isotopic work. Bull.-Geol. Surv. Japan 30, 241–245.

Schmidt, C.J., Smedes, H.W., O'Neill, J.M., 1990. Syncompressional emplacement of the Boulder and Tobacco Root batholiths (Montana, USA) by pull-apart along old fault zones. Geol. J. 25, 305–318.

Seal II, R.R., Alpers, C.N., Rye, R.O., 2000. Stable isotope systematics of sulfate minerals. In: Alpers, C.N., Jambor, J.L., Nordstrom, D.K. (Eds.), Sulfate Minerals—Crystallography, Geochemistry, and Environmental Significance, Rev. Mineral. Geochem., vol. 40, pp. 541–602.

Sha, Lian-Kun, Chappell, B.W., 1999. Apatite chemical compositions, determined by electron microprobe and laser-ablation inductively coupled plasma mass spectrometry, as a probe into granite petrogenesis. Geochim. Cosmochim. Acta 63, 3861–3881.

Sheppard, S.M.F., Taylor Jr., H.P., 1974. Hydrogen and oxygen isotope evidence for the origin of water in the Boulder Batholith and Butte ore deposits, Montana. Econ. Geol. 69, 926–946.

Smedes, H.W., 1966. Geology and igneous petrology of the Northern Elkhorn Mountains, Jefferson and Broadwater counties, Montana. U. S. Geol. Surv. Prof. Pap. 510, 116.

Smith, A.G., Barnes, W.C., 1966. Comparison of and facies changes in the carbonaceous, calcareous and dolomitic formations of the Precambrian Belt Supergroup. Geol. Soc. Amer. Bull. 77, 1399–1426.

Snee, L., Miggins, D., Geissman, J., Reed, M., Dilles, J., Zhang, L., 1999. Thermal history of the Butte porphyry system, Montana. Abstr. Programs-Geol. Soc. Am. 31 (7), A380.

Stearn, C.W., Carroll, R.L., Clark, T.H., 1979. Geological Evolution of North America. Wiley, New York.

Strauss, H., Scheiber, J., 1990. A sulfur isotope study of pyrite genesis; the mid-Proterozoic Newland Formation, Belt Supergroup, Montana. Geochim. Cosmochim. Acta 54, 197–204.

Streck, M.J., Dilles, J.H., 1998. Sulfur evolution of oxidized arc magmas as recorded in apatite from a porphyry copper batholith. Geology 26, 523–526.

Taylor Jr., H.P., 1997. Oxygen and hydrogen isotope relationships in hydrothermal mineral deposits. In: Barnes, H.L. (Ed.), Geochemistry of Hydrothermal Ore Deposits, (3rd ed.)Wiley, New York, pp. 229–302.

Thode, H.G., Monster, J., Dunford, H.B., 1961. Sulphur isotope geochemistry. Geochim. Cosmochim. Acta 25, 159–174.

Tilling, R.I., 1964. Variation in modes and norms of a "homogeneous" pluton of the Boulder Batholith, Montana. U. S. Geol. Surv. Prof. Pap. 501-D, D8–D15.

Ulrich, T., Günther, D., Heinrich, C.A., 2001. The evolution of a porphyry Cu–Au deposit, based on LA-ICP-MS analysis of fluid inclusions: Bajo de la Alumbrera, Argentina. Econ. Geol. 96, 1743–1774.

Weed, W.H., 1912. Geology and ore deposits of the Butte distict, Montana. U. S. Geol. Surv. Prof. Pap., 74.

Whitney, J.A., 1984. Volatiles in magmatic systems. In: Robertson, J.M. (Ed.), Fluid–Mineral Equilibria in Hydrothermal Systems, Rev. Econ. Geol., vol. 1, pp. 155–175.

Wones, D.R., 1989. Significance of the assemblage titanite+magnetite+quartz in granitic rocks. Am. Mineral. 74, 744–749.

Zhang, Lihua, 2000. Stable isotope investigation of a hydrothermal alteration system—Butte porphyry copper deposit. PhD thesis, Oregon State University, Corvallis.

Zhang, Lihua, Field, C.W., Dilles, J.H., Reed, M.H., 1999. Sulfur isotope record of deep porphyry Cu–Mo mineralization, Butte District, Montana. Abstr. Programs-Geol. Soc. Am. 31 (7), A381–A382.